Organic & Biomolecular Chemistry

ROYAL SOCIETY OF CHEMISTRY

REVIEW

View Article Online
View Journal | View Issue

Check for updates

Cite this: *Org. Biomol. Chem.*, 2025, **23**, 2756

Pretzelanes, [1]rotaxanes and molecular figures-of-eight – crossing the bridge from fundamentals to functional applications

Rebecca L. Spicer and Nicholas H. Evans *

Received 8th January 2025,
Accepted 6th February 2025

DOI: 10.1039/d5ob00031a

rsc.li/obc

There are myriad [2]catenanes and [2]rotaxanes that consist of two interlocked molecular components. On occasion, supramolecular chemists prepare interlocked molecules where there are covalent linkages between the interlocked molecular components. In this review, progress on pretzelanes ([1]catenanes), [1]rotaxanes and molecular figures-of-eight is surveyed. Particular attention is paid to the application of such molecules, especially where the interlocked structure and/or the covalent linkage(s) play a key functional role.

Open Access Article. Published on 12 February 2025. Downloaded on 2/9/2026 7:36:12 PM.
This article is licensed under a Creative Commons Attribution 3.0 Unported Licence.

Introduction

The archetypal examples of mechanically interlocked molecules (MIMs), [2]catenanes[1] (Fig. 1a) and [2]rotaxanes[2] (Fig. 1b) are most celebrated for the possibility of controlled molecular motion of their interlocked components and that property being deployed in "molecular machines".[3] Static and dynamic [2]catenanes and [2]rotaxanes (and on occasion higher order MIMs containing more than two interlocked components) have been deployed in a range of useful host–guest applications, *e.g.* as hosts for ionic guests[4] and as catalysts for reactions.[5] Within this research activity, an area of particular current interest is the study of chiral MIMs.[6]

In a [2]catenane or [2]rotaxane there is no covalent bond between the interlocked components. Formation of these MIMs is typically achieved by use of non-covalent template synthesis where precursor components are self-assembled by metal cation,[7] π–π stacking (or aromatic donor–acceptor interactions),[8] hydrogen bonding[9] and/or other non-covalent interaction(s) before covalent bond formation traps the interlocked structure. However, if a covalent link is installed between the two rings of a [2]catenane this will lead to a *[1]catenane*, typically referred to as a *pretzelane* (Fig. 1c). The analogous process as applied once to the ring and axle of a [2]rotaxane leads to a

Department of Chemistry, Lancaster University, Lancaster, LA1 4YB, UK.
E-mail: n.h.evans@lancaster.ac.uk

Rebecca L. Spicer

Bec Spicer graduated with a First Class Masters in Chemistry from the University of St Andrews in 2015. She then moved to Prof Paul Lusby's laboratory at the University of Edinburgh, completing a PhD thesis on coordination capsule catalyzed organic transformations. In 2020, Bec moved to Lancaster University, where she has undertaken postdoctoral research on [1]rotaxanes inspired by lasso peptides. During 2024, she commenced a Leverhulme Trust Early Career Fellowship at Lancaster University.

Nicholas H. Evans

Nick Evans graduated from Wadham College, University of Oxford with a First Class Masters in Chemistry (2006) and DPhil in Inorganic Chemistry (2011), having worked on anion sensing rotaxanes and catenanes under the supervision of Prof Paul Beer. Nick then undertook postdoctoral research on lanthanide complexes with Prof David Parker at Durham University. In 2013, Nick commenced his independent academic career at Lancaster University, where he is currently Senior Lecturer and Head of Department. His research interests are in functional supramolecular chemistry, seeking to exploit mechanically interlocked molecules in useful applications.

This journal is © The Royal Society of Chemistry 2025

Open Access Article. Published on 12 February 2025. Downloaded on 2/9/2026 7:36:12 PM.
This article is licensed under a Creative Commons Attribution 3.0 Unported Licence.

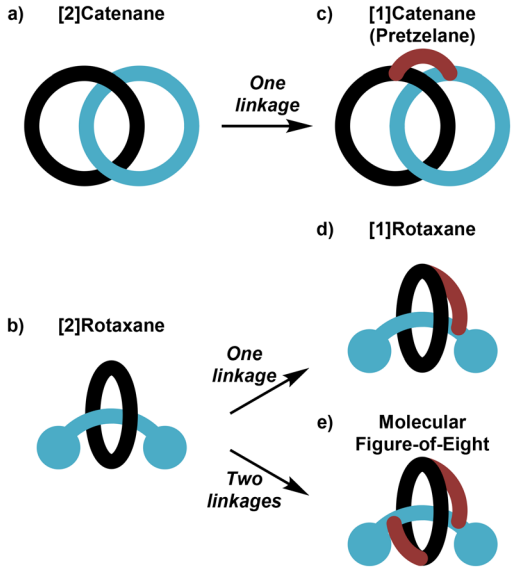

Fig. 1 Schematic representation of (a) [2]catenane; (b) [2]rotaxane; (c) pretzelane (or [1]catenane); (d) [1]rotaxane; (e) molecular figure-of-eight.

[1]rotaxane (Fig. 1d); if applied appropriately twice it may lead to a *molecular figure-of-eight* (Fig. 1e).[10]

Pretzelanes, [1]rotaxanes and molecular figures-of-eight are not simply synthetic chemistry curiosities. It is well-established that the family of bacterially produced *lasso peptides* – many of which have useful therapeutically relevant properties – include structural types based upon [1]rotaxane (*Class II*) and figure-of-eight (*Class III*) architectures.[11] Meanwhile, systematic screening of the Protein Data Bank (PDB) has identified several single chain proteins possessing pretzelane structures.[12]

Here we set out progress in the synthesis of pretzelanes, [1]rotaxanes and molecular figures-of-eight. Attention is paid to where inclusion of covalent link(s) allows for control of the conformational behaviour of the interlocked components of the MIM and/or otherwise affects the properties thereof. We discuss the performance of bridged MIMs that have been used in functional applications, specifically concluding with examples inspired by lasso peptides. We do not aim to be exhaustive, instead we illustrate and exemplify using a selection of significant contributions in the field. We also avoid discussion of related "higher order" systems, such as molecular daisy chains.[13–17]

Pretzelanes

Pretzelanes may be prepared by covalently linking or "bridging" the two interlocked rings of a [2]catenane (Fig. 2a). However, there is an alternative templated self-assembly strategy, where the interlocked macrocyclic rings are "clipped" shut using tethered macrocycle precursor(s) (Fig. 2b). Pretzelanes (including the first known examples) are also to be found as intermediates in the preparation of [2]catenanes by directed covalent synthesis.

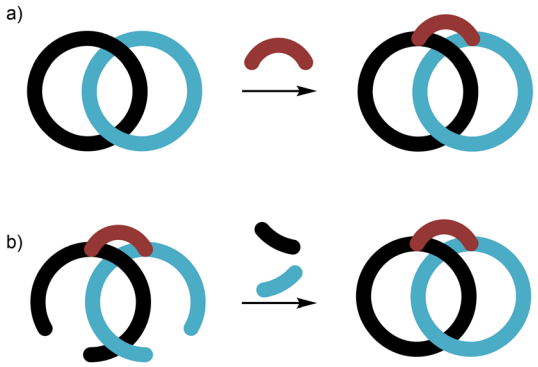

Fig. 2 Schematic representation of synthetic routes to pretzelanes: (a) "bridging" the rings of a [2]catenane; (b) "clipping" shut self-assembled tethered macrocycle precursor(s).

Pretzelanes arising from bridging the rings of [2]catenanes

Vögtle and co-workers prepared several pretzelanes from [2]catenanes synthesized *via* hydrogen bond templation.[18–21] Their first example, **1**, was synthesized by reacting the parent [2]catenane with the appropriate di-iodo compound in the presence of base (K_2CO_3) to deprotonate the acidic sulfonamides, under diluted reaction conditions (Fig. 3).[18] This pretzelane is chiral, through the rotational asymmetry of the interlocked rings. In collaboration with Okamoto, a sample of the pretzelane was resolved by chiral HPLC, with pronounced Cotton effects being observed in the aromatic chromophore region of the CD spectrum.[19]

In follow-up work, Vögtle and co-workers studied the length of an alkyl bridge when preparing pretzelanes **2** from a related [2]catenane (Fig. 3).[20] Decreasing the length of the bridge from 10 to 6 methylene units, resulted in a decrease of yield from 47% to 5% for the bridging reaction. Separating the enantiomers of these pretzelanes by chiral HPLC proved challenging;

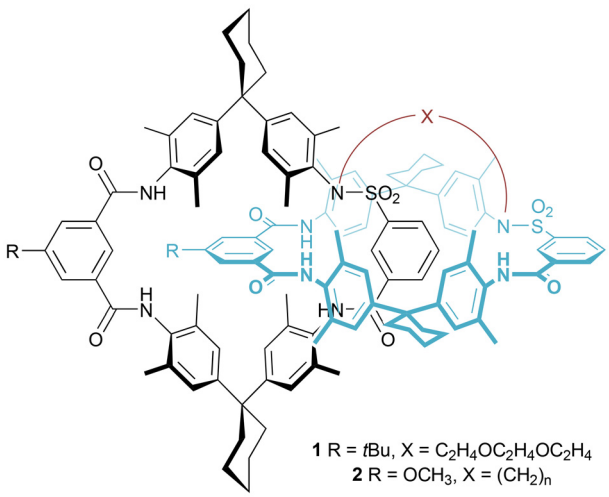

Fig. 3 Vögtle's pretzelanes prepared from bridging rings of hydrogen bond templated [2]catenanes.

Open Access Article. Published on 12 February 2025. Downloaded on 2/9/2026 7:36:12 PM.
This article is licensed under a Creative Commons Attribution 3.0 Unported Licence.

for the two examples where this was achieved (10 and 8 methylene units), the Cotton effect observed in the CD spectrum was lower for the pretzelane with the shorter bridge.

A pretzelane arises from an interesting study by Shimada, Ishikawa and Tamaoki (Fig. 4).[22] The researchers synthesized a classical Sauvage-style [2]catenane using phenanthroline ligands and a Cu(I) template. Both rings of [2]catenane **3** possess benzyloxycarbonyl (Cbz) protected secondary amines. The [2]catenane was isolated free of the Cu cation template and the Cbz protecting groups removed. Reaction of the free amines with adipoyl chloride furnished pretzelane **4** in an impressive 78% yield for the bridging reaction. In contrast, if the [2]catenane was re-metallated with Cu(I), the reaction with adipoyl chloride led to formation of a polymer chain.

Pretzelanes arising from clipping shut self-assembled tethered macrocycle precursors

By use of π–π stacking (alternatively termed aromatic acceptor-donor interactions), Stoddart and co-workers prepared pretzelanes by clipping shut a covalently linked macrocycle and macrocycle precursor.[23] Specifically, the self-assembly of electron-poor bis-pyridinium **6** around the electron-rich naphthalene of crown ether macrocycle **5**, allowed for generation of pretzelane **7** (in 49% yield) by reaction of the terminal pyridine functionality of **6** with the di-benzyl phthalimide of **5** (Fig. 5). With a shorter linker between crown ether and phthalimide, a pretzelane was obtained in 14% yield, with a "higher order" cyclic bis[2]catenane isolated in 20% yield.

These pretzelanes exhibit helical chirality, arising from location of the crown ether on either one of the two bipyridiniums. In subsequent work, the inclusion of a classical stereogenic centre in the linker led to a marked preference for one conformational diastereoisomer of pretzelane **8**, computationally modelled to be the *M*, rather than *P*, isomer (Fig. 6a).[24] Notably, a significant CD response arises in the charge transfer region and the bipyridinium absorption. Thus, a stereogenic centre in the linker provides a detectable chiral influence elsewhere in the pretzelane.

Alternatively, incorporation of tetrathiafulvalene (TTF) enabled formation of a bistable pretzelane **9** (Fig. 6b).[25] Upon single electron oxidation of the TTF to the TTF radical cation, the positively charged tetrapyridinium ring translates to the 1,5-dioxynaphthalene motif. Upon reduction of the TTF

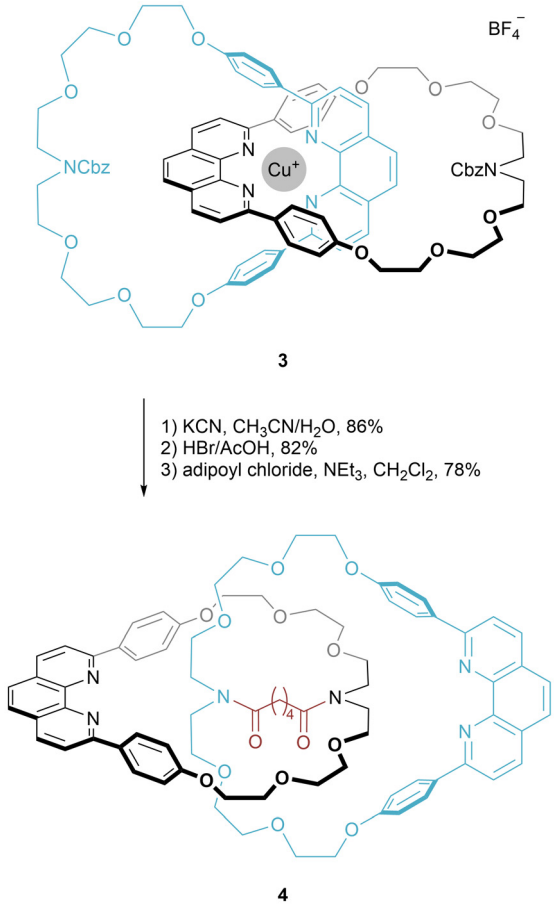

Fig. 4 Shimada and Tamaoki's synthesis of a pretzelane prepared from a demetallated Sauvage-style [2]catenane.

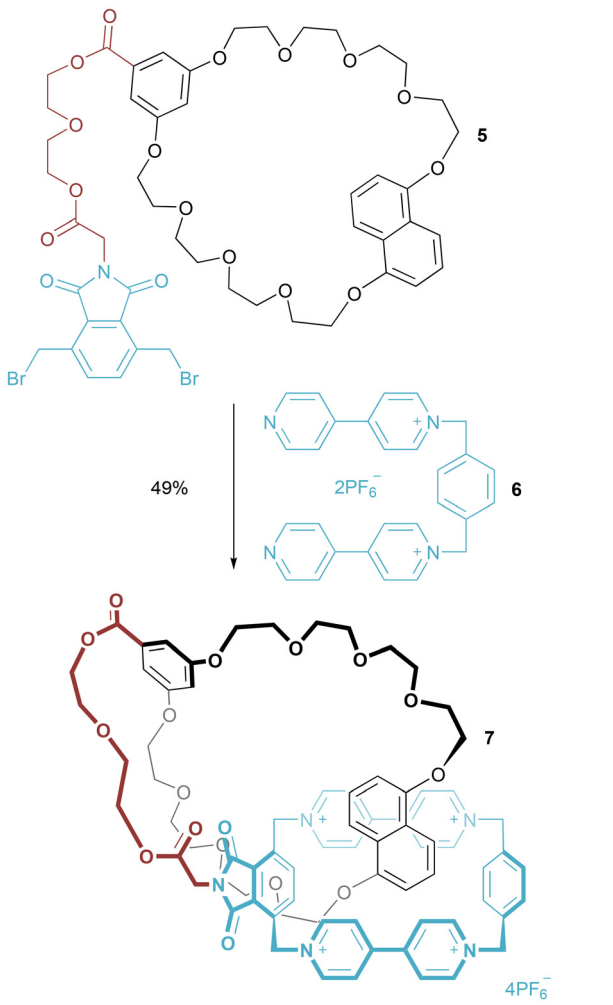

Fig. 5 Stoddart's first synthesis of a pretzelane prepared by π–π stacking templation (NB: *P* isomer of pretzelane **7** depicted).

This journal is © The Royal Society of Chemistry 2025

Open Access Article. Published on 12 February 2025. Downloaded on 2/9/2026 7:36:12 PM.
This article is licensed under a Creative Commons Attribution 3.0 Unported Licence.

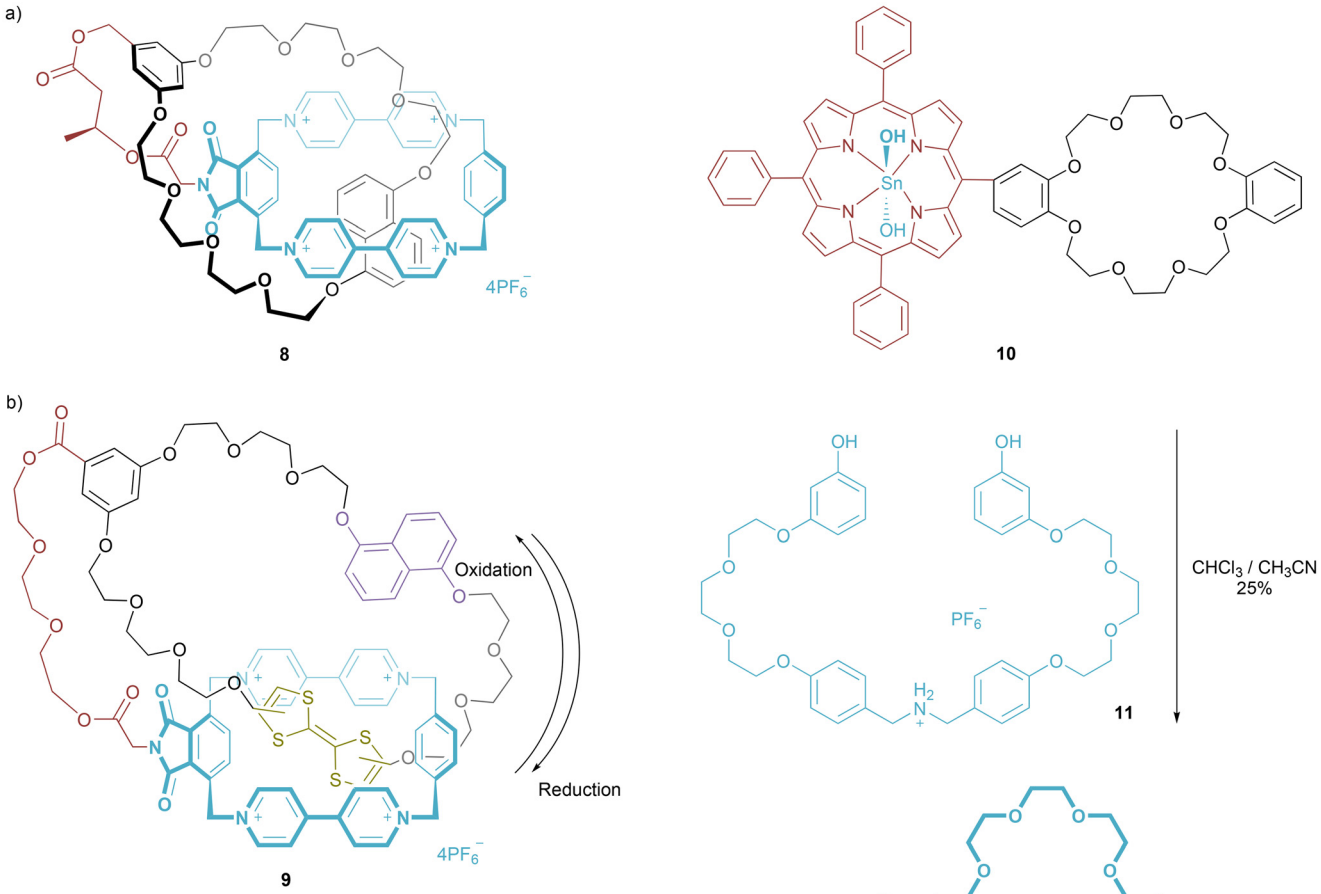

Fig. 6 Structures of (a) Stoddart's substituted pretzelane demonstrating a conformational preference for *M* helical chirality; (b) Stoddart's bistable pretzelane switchable by oxidation and reduction of the tetrathiafulvalene (TTF) motif.

radical cation/dication, there exists a metastable conformation (detectable by CV) before return of the tetrapyridinium ring to its initial position over the TTF moiety. The authors highlight that due to the linker this motion is unidirectional (in contrast to the equivalent [2]catenane).[26]

An intriguing example of ring clipping was reported by Liu and co-workers giving a structurally unusual pretzelane (Fig. 7).[27] The threading of a macrocycle precursor through the dibenzo-24-crown ether was promoted through the hydrogen bonding interactions between the ammonium cation (**11**) and ether oxygens (**10**). The hydroxy groups at the termini of the threading component **11** were then able to undergo axial ligation of the Sn-porphyrin dihydroxide of **10** to give the interlocked architecture **12** in 25% yield.

Fig. 7 Liu's synthesis of a pretzelane using electrostatically augmented hydrogen bond templation.

Pretzelanes arising as intermediates in the covalent directed synthesis of [2]catenanes

Pre-dating the work above, pretzelanes were encountered in Schill's ground-breaking work on the directed covalent synthesis of [2]catenanes (Fig. 8).[28] Double intramolecular alkylation of **13** generates double bridged species **14**. Cleavage of the cyclic ketal creates pretzelane **15** containing a single bond link between the two rings. Subsequent oxidation and hydrolysis of this bond formed the interlocked but not covalently linked rings of [2]catenane **16**.

Subsequently, Godt prepared a [2]catenane by use of a diphenylcarbonate covalent template.[29] The intermediate pretzelane **17** (Fig. 9) was prepared by clipping shut a macrocyclic ring by alkyne-alkyne coupling. Cleavage of the diphenylcarbonate bridge (by use of TBAF) yielded the desired [2]catenane in 63% yield.

We also choose to highlight an example from the recent work of van Maarseveen, who has revived the field of covalent directed synthesis of interlocked molecules.[30]

Open Access Article. Published on 12 February 2025. Downloaded on 2/9/2026 7:36:12 PM.
This article is licensed under a Creative Commons Attribution 3.0 Unported Licence.

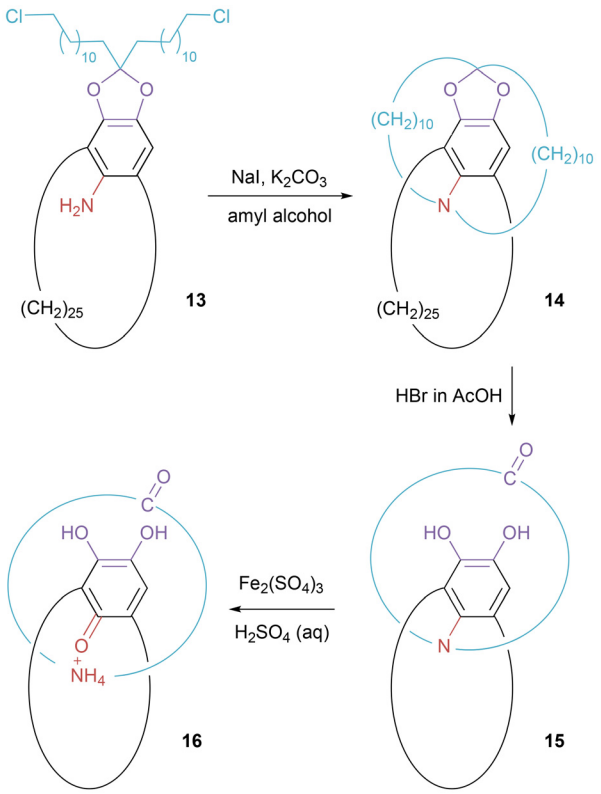

Fig. 8 Schematic representation of Schill's [2]catenane synthesis that proceeds through an intermediate pretzelane.

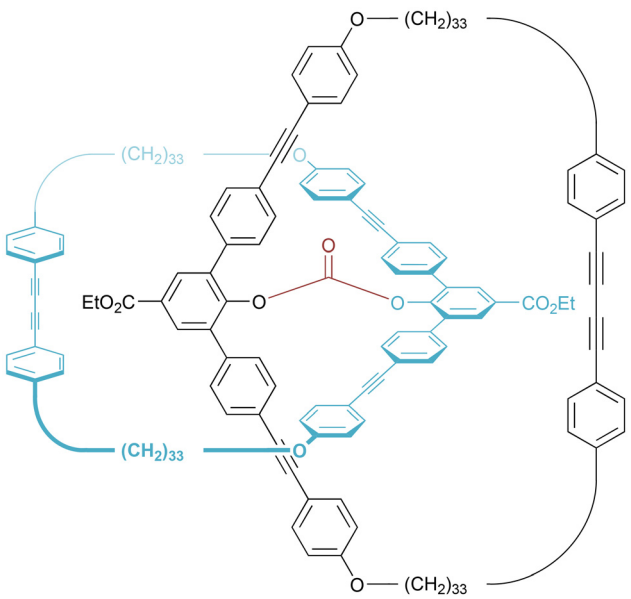

Fig. 9 The intermediate pretzelane in Godt's synthesis of a [2]catenane.

Cleavage of covalent straps in the multiply bridged **18** yielded "quasi[1]catenane" **19**, which may be converted to [2]catenane **20** by ketal hydrolysis (Fig. 10).[31] It should be emphasized that

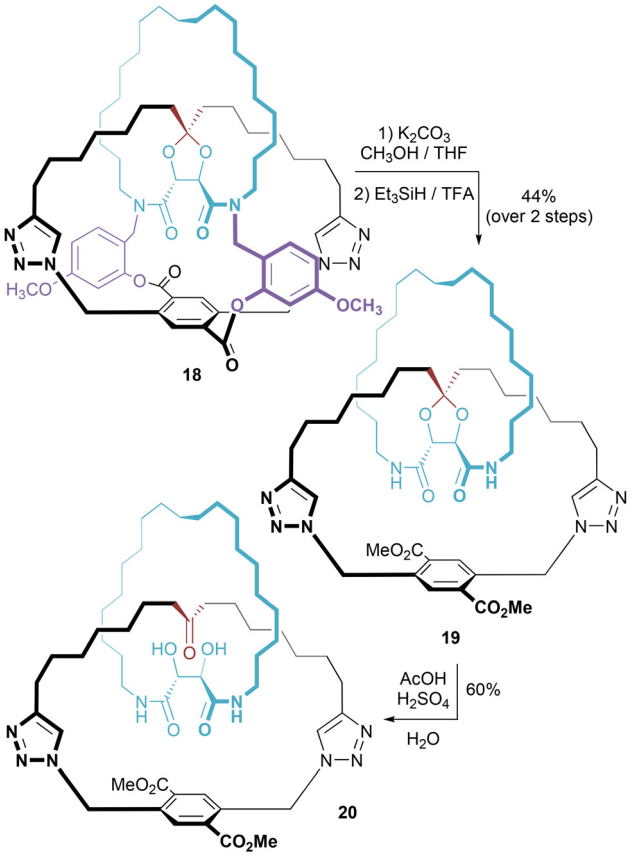

Fig. 10 van Maarseveen's synthesis of a [2]catenane that proceeds through an intermediate "quasi[1]catenane".

19 is not strictly a pretzelane for the two rings are not bridged but are connected at a single atom.

[1]Rotaxanes

While the [1]rotaxane in Fig. 1d possesses two bulky stopper groups on its axle component (being derived from a [2]rotaxane), it might be thought that a [1]rotaxane may only require a single stopper group at the terminus of the threaded axle. However, it is important to appreciate the potential for a single-stoppered pseudo[1]rotaxane structure to disentangle by "tumbling" as illustrated in Fig. 11.[32] To prevent this process, either a bulky internal functional group, a sufficiently inflexible pivot or some other means is required to create a permanently stable structure. For simplicity, we will focus the scope of this review on [1]rotaxanes that are truly mechanically interlocked.

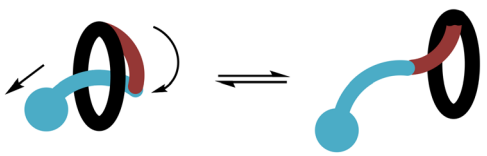

Fig. 11 Schematic representation of a pseudo[1]rotaxane structure disentangling by "tumbling".

This journal is © The Royal Society of Chemistry 2025

Open Access Article. Published on 12 February 2025. Downloaded on 2/9/2026 7:36:12 PM.
This article is licensed under a Creative Commons Attribution 3.0 Unported Licence.

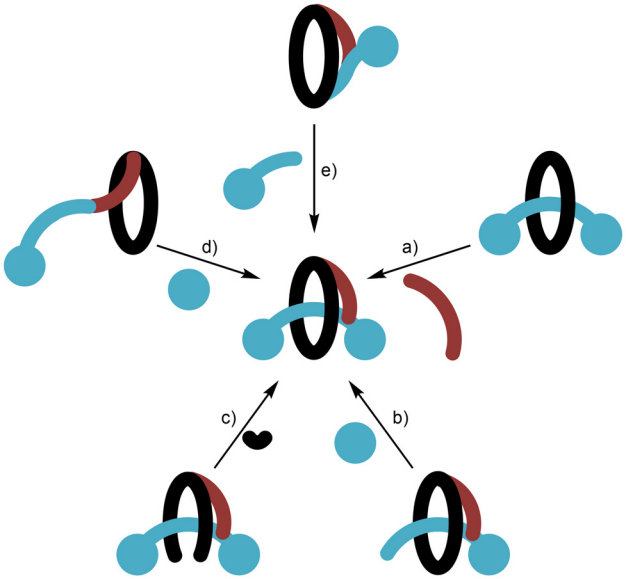

Fig. 12 Schematic representation of synthetic routes to permanently entangled [1]rotaxanes: (a) covalently linking ring and axle; (b) threading and stoppering; (c) clipping shut; (d) entanglement and stoppering; (e) directed covalent approach. NB: *in lieu* of a second stopper, a [1]rotaxane may be permanently entangled by inclusion of a sufficiently inflexible pivot.

The principal synthetic strategies to prepare [1]rotaxanes are listed below and illustrated in Fig. 12.[33]

(a) Covalently linking the ring and axle of a [2]rotaxane;
(b) Threading and stoppering;
(c) Clipping shut;
(d) Entanglement and stoppering;
(e) Directed covalent approach.

[1]Rotaxanes prepared by covalently linking the ring and axle of [2]rotaxanes

Analogous to the preparation of pretzelanes, Vögtle demonstrated that incorporation of acidic sulfonamide groups into the ring and axle components of a hydrogen bond templated [2]rotaxane allows for bridging by alkylation to generate [1]rotaxanes **21** (Fig. 13). The first example, X = $C_2H_4OC_2H_4OC_2H_4$, was produced in a very respectable 71% yield.[34] As for the pretzelane, the [1]rotaxane is chiral, and it was possible to resolve using chiral HPLC, to allow for the recording of CD spectra of the two enantiomers.[19]

Further study focused on varying the length of the bridge (X = $(CH_2)_n$).[20] No general trend was observed between yield of bridging reaction and length of the bridge (between 1 and 10 methylene units). Of the eight isolated examples – seven were resolvable by chiral HPLC. In CD spectroscopy studies, Cotton effects decreased as the length of the bridge decreased.

Benzylic bridges were also investigated.[35] [1]Rotaxanes were isolated in good yields, with crystal structures being obtained. Resolution of four out of six examples by chiral HPLC was possible. An increase in molar CD by a factor of two (in comparison to aliphatic bridged [1]rotaxanes) was attributed to the chromophoric character of the bridges and the reduced flexibility of these [1]rotaxanes.

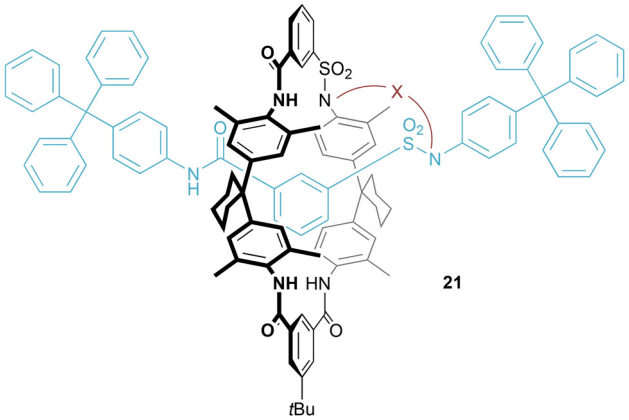

Fig. 13 Generic structure of Vögtle's [1]rotaxane prepared from bridging between ring and axle of a hydrogen bond templated [2]rotaxane.

Zhou and Yan reported upon the covalent bridging of [2]rotaxane **22** which had been synthesized by electrostatically augmented hydrogen bond templation (Fig. 14).[36] The benzo-21-crown-7 macrocyclic ring is advantageous compared to the more commonly encountered dibenzo-24-crown-8, because the 21-crown-7 is sufficiently small to allow the benzene rings in the axle component to be bulky enough to act as stoppers. Axle and macrocycle were covalently linked together using Eglinton coupling to form [1]rotaxane **23**, with related **24** prepared by hydrogenation. Unsurprisingly, [1]rotaxane **24** with a more flexible all sp^3 linker has more rotational motions (as detected by variable temperature NMR experiments) than [1]rotaxane **23** with its linker containing sp hybridized atoms.

Easton and co-workers synthesized α-cyclodextrin [2]rotaxanes **25** and [1]rotaxanes **26** by exploitation of the hydrophobic effect (Fig. 15).[37] In the [2]rotaxanes, the cyclodextrin macrocycle is free to pirouette around the axle, on the NMR timescale. However, in the [1]rotaxanes the succinamide link reduces rotation – most notably in the case where R = OCH_3, with the authors describing a so-called "ratchet tooth and pawl" mechanism arising from clash of the methoxy substituent and the succinamide linker.

[1]Rotaxanes prepared by threading and stoppering

It has been demonstrated that the two cyclopentadienyl rings of ferrocene can act as sites of linkage between the macrocyclic ring and axle components of [1]rotaxanes.[38,39] For example, Qu's [1]rotaxane **27** prepared by electrostatically augmented hydrogen bond templated threading followed by stoppering using the CuAAC "click" reaction and subsequent methylation of the resulting triazole (Fig. 16).[38] Deprotonation of the ammonium leads to translation of the ring to the positively charged triazolium, as first demonstrated in [2]rotaxanes by Coutrot.[40] This event is accompanied by an alteration in the electrochemical properties of the [1]rotaxane – the free amine leads to loss in reversibility of the Fc/Fc^+ redox couple.

Open Access Article. Published on 12 February 2025. Downloaded on 2/9/2026 7:36:12 PM.
This article is licensed under a Creative Commons Attribution 3.0 Unported Licence.

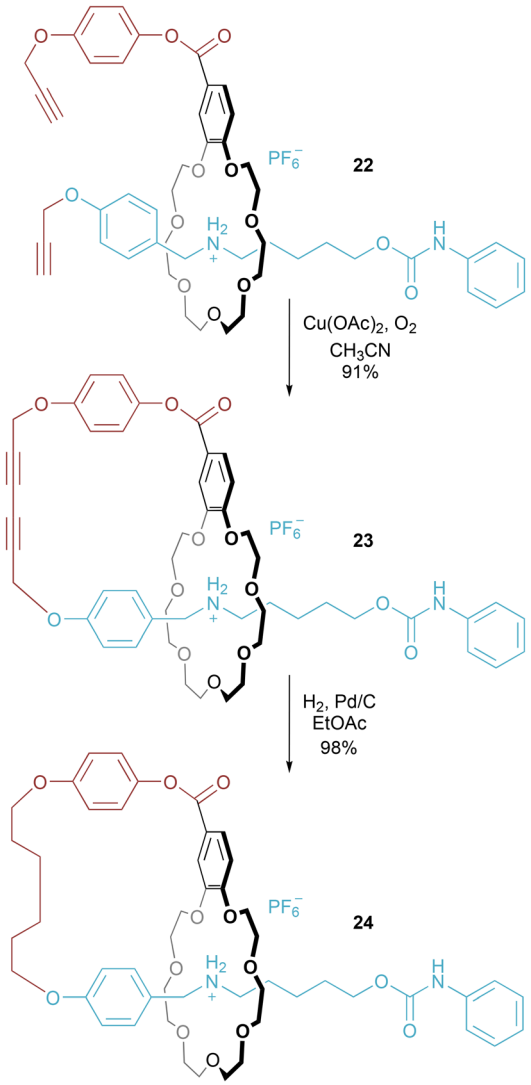

Fig. 14 Zhou and Yan's synthesis of crown ether/secondary ammonium [1]rotaxanes.

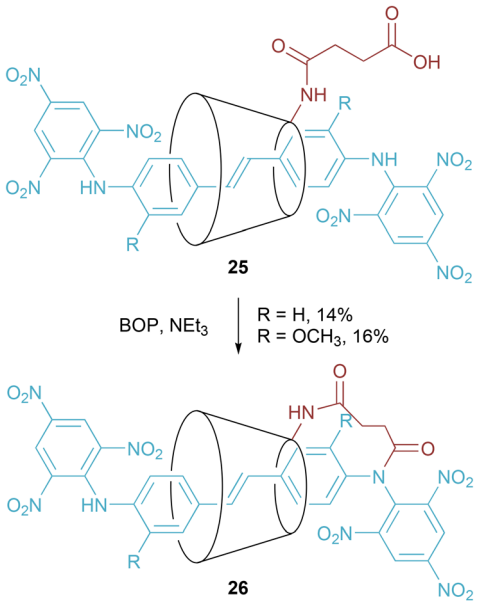

Fig. 15 Easton's synthesis of [1]rotaxanes that exhibit restricted pirouetting of the cyclodextrin ring.

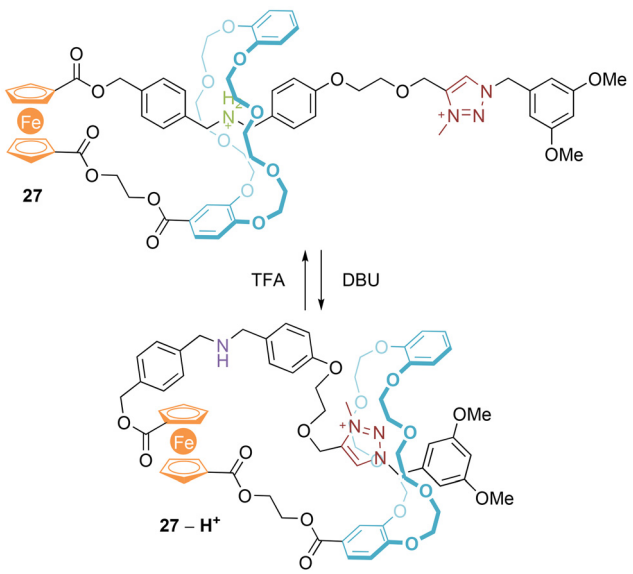

Fig. 16 Qu's first ferrocene containing switchable [1]rotaxane (NB: counter-anions not included to avoid ambiguity).

Subsequently, related [1]rotaxane **28** was prepared incorporating a naphthalimide (NDI) (Fig. 17).[39] Addition of DBU results in motion of the ring from the ammonium/amine station to the triazolium, and quenching of NDI fluorescence due to photoinduced electron transfer (PET) between the electron rich ferrocene and the electron deficient NDI fluorophore. The translation is reversible with addition of TFA, accompanied by restoration of fluorescence. However, in the presence of $Fe(ClO_4)_3$, no quenching of fluorescence is observed upon addition of DBU, consistent with oxidation of the ferrocene to ferrocenium.

A particularly notable example from Qu's laboratory deploys a crowded olefin motor to pump ring-sliding using light (Fig. 18).[41] [1]Rotaxane **29**, prepared by an analogous synthetic strategy to the previous ferrocene containing examples, incorporates a second generation Feringa-style light-driven molecular motor. Following deprotonation of the templating secondary ammonium, controlled translational motion of the crown ether macrocycle along the axle of the [1]rotaxane is possible by photoinduced *cis*-to-*trans* isomerization and thermal helix inversion of the crowded olefin motor.

Exciting proof-of-principle photophysical applications of [1]rotaxanes have recently been demonstrated by Lin and coworkers.[42,43] For example, they prepared a Coutrot-style bistable [1]rotaxane **30** containing a tetraphenylene (TPE) donor and photochromic diarylethene (DAE) acceptor (Fig. 19).[42] As expected, pH-controlled shuttling between con-

This journal is © The Royal Society of Chemistry 2025

Open Access Article. Published on 12 February 2025. Downloaded on 2/9/2026 7:36:12 PM.
This article is licensed under a Creative Commons Attribution 3.0 Unported Licence.

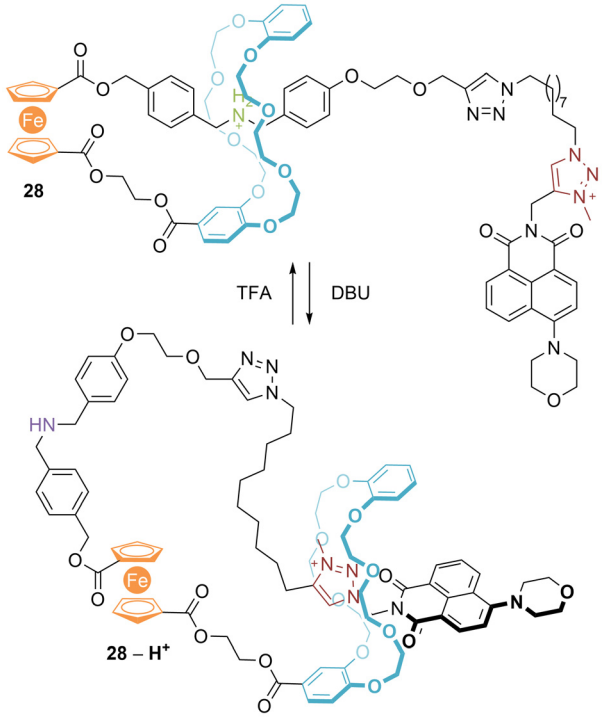

Fig. 17 Qu's ferrocene containing switchable [1]rotaxane with a controllable fluorescence signal (NB: counter-anions not included to avoid ambiguity).

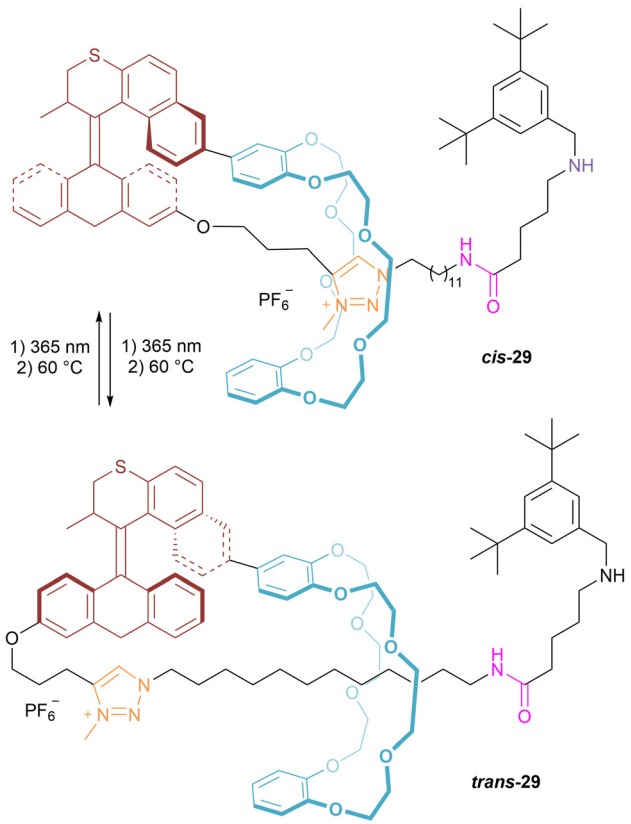

Fig. 18 Operation of Qu's light-driven [1]rotaxane pump.

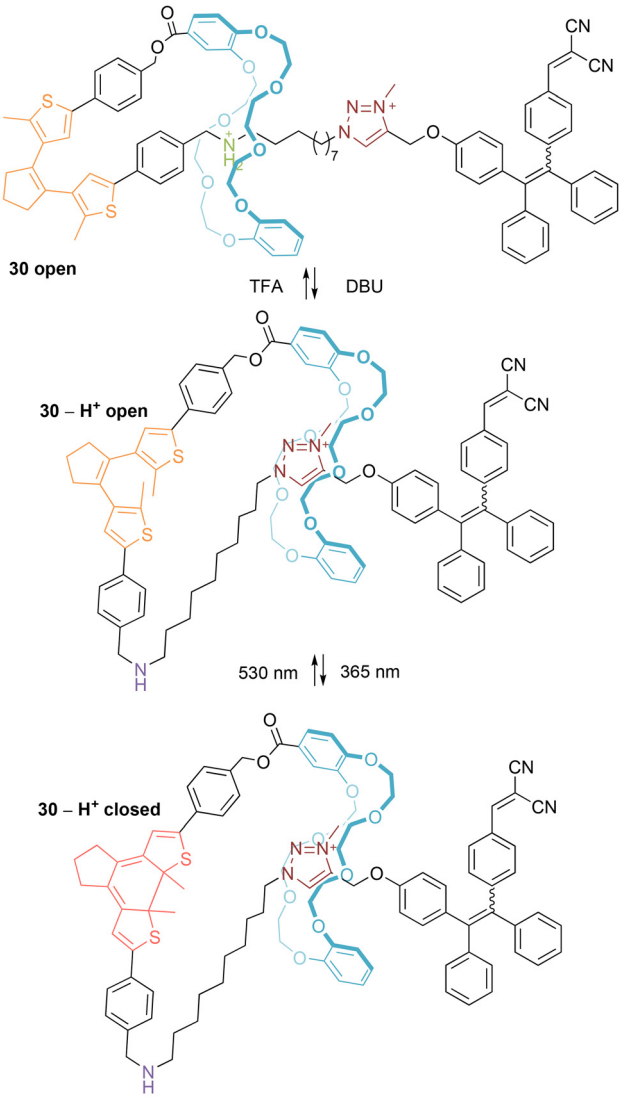

Fig. 19 Operation of Lin's switchable TPE/DAE [1]rotaxane for controlled singlet oxygen generation (NB: counter-anions not included to avoid ambiguity).

tracted/extended conformers occurs. When **30** is in the contracted conformer, Förster Resonance Energy Transfer (FRET) is not possible, and the DAE acceptor is unable to photoisomerize between open and closed forms. In contrast, the extended conformer of **30** (as well as the non-interlocked isomer) has switchable FRET, activated by dual and sequential pH- and photo-switching. Impressively, surface modified nanoparticles incorporating the [1]rotaxane have been prepared that demonstrate controllable generation of singlet oxygen in cells (possible when the DAE acceptor is in its open form), hinting at potential real-world application of this system.

In another report, Lin describes the incorporation of *N*,*N*′-diphenyl-dihydrodibenzo[*a*,*c*]phenazine (DPAC), a vibration induced emission (VIE) fluorophore, into a Coutrot-style acid/base switchable [1]rotaxane **31** (Fig. 20).[43] While a non-interlocked analogue generates orange emission, for the tightened

Open Access Article. Published on 12 February 2025. Downloaded on 2/9/2026 7:36:12 PM.
This article is licensed under a Creative Commons Attribution 3.0 Unported Licence.

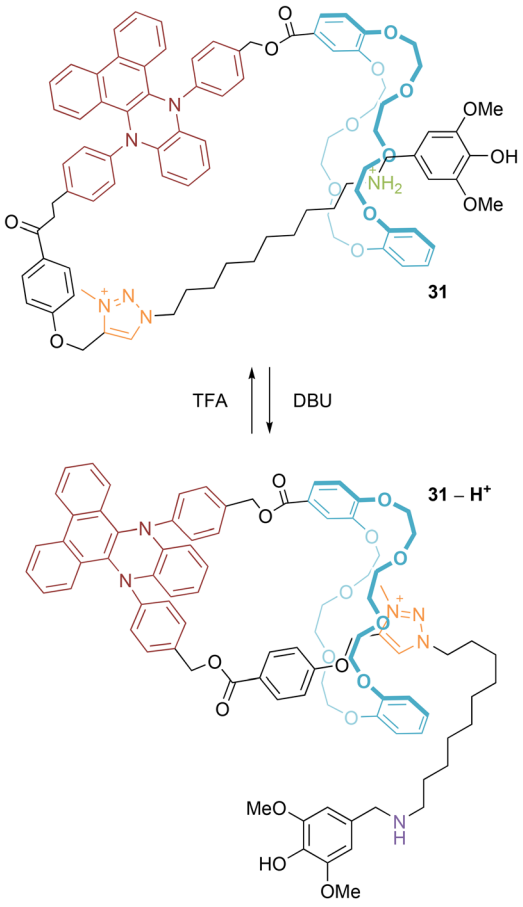

Fig. 20 Lin's switchable DPAC containing [1]rotaxane. (NB: counter-anions not included to avoid ambiguity).

conformation of [1]rotaxane **31** with the crown ether at the triazolium station, there is blue emission due to the large conformational restraint upon the DPAC moiety. If the crown ether is at the templating ammonium station, a mix of blue and orange emission is possible, tunable by adjusting the viscosity and polarity of the solvent, as well as temperature, allowing access to white light emission. Alternatively, the variable emission properties of the loosened conformation of **31** can be used as a sensor of solvent viscosity and/or temperature.

Tian and researchers prepared [1]rotaxane **33** through self-inclusion of azobenzene-modified β-cyclodextrin **32** followed by capping by Suzuki coupling in aqueous solution (Fig. 21).[44] By application of different wavelengths of light, switching of the azo bond between *E* and *Z* isomers enforces relative motion of the axle and macrocyclic components.[45]

Recently, the laboratories of Zhu, Tian and Liu have shown [1]rotaxane cyclodextrin **35** may provide solvent and temperature dependent circularly polarized luminescence (CPL) responses (Fig. 22).[46] Consisting of a dansyl emitter and an inherently chiral β-CD macrocycle, [1]rotaxane **35** exhibits solvent dependent CPL behaviour as a free molecule in solution. This was rationalized by ^{1}H NMR spectra revealing conformers with different degrees of dansyl inclusion within the

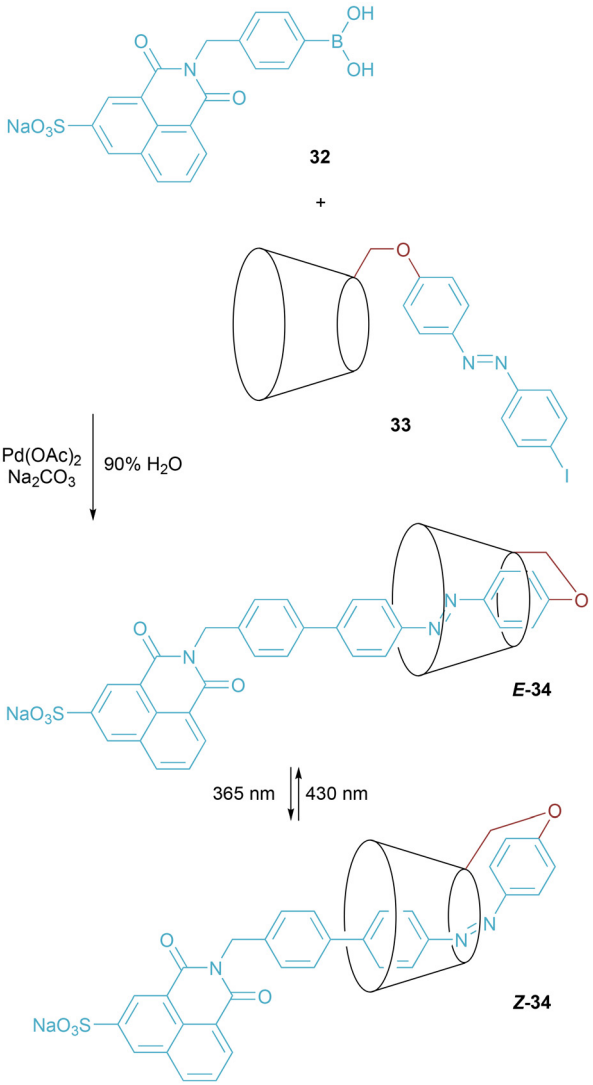

Fig. 21 Tian's synthesis of a cyclodextrin containing switchable [1]rotaxane.

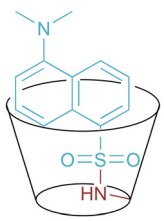

Fig. 22 Structure of dansyl functionalized β-cyclodextrin [1]rotaxane.

CD cavity. When allowed to self-assemble into an extended "channel" architecture, a thermo-amplified CPL response is detectable, with both high quantum yield and luminescence dissymmetry factor observed.

Han and Chen reported a helic[6]arene-based chiral [1]rotaxane **38** prepared by alkylation of a tethered tertiary

This journal is © The Royal Society of Chemistry 2025

Open Access Article. Published on 12 February 2025. Downloaded on 2/9/2026 7:36:12 PM.
This article is licensed under a Creative Commons Attribution 3.0 Unported Licence.

amine thread (**36**) with benzyl-bromide tetraphenylethene derivative **37**, a reaction which in chloroform proceeded in an excellent yield of 98% (Fig. 23).[47] In the CD spectrum, signals appear at 310–340 nm, attributed to chirality transfer from the enantiopure helic[6]arene to the TPE moiety, which was not observed for the unthreaded isomer.

A pillar[5]arene-based [1]rotaxane **41** was prepared by Wang, Chen, Han, Yao and co-workers by stoppering a self-threaded precursor **39** (Fig. 24).[48] When Zn(II) is added to a chloroform/methanol solution of **41**, there is a dramatic fluorescence enhancement, with it being proposed that a 2 : 1 rotaxane/cation binding event is occurring at the salicyldiamine stopper group (inset of Fig. 25). Demonstration of a detection limit of 10^{-7} M for aqueous Zn cations has also been achieved for a solid-phase sensor prepared by drop-casting a solution of **41** onto a glass slide.[49]

A covalent stereogenic centre attached to a rotationally unsymmetrical macrocycle can direct the diastereoselective synthesis of mechanically chiral [1]rotaxanes prepared using CuAAC active metal templation (Fig. 25).[50] In a thorough study to maximize formation of the interlocked [1]rotaxane **45**, Papot and co-workers identified the addition of macrocycle **44** as being beneficial in ensuring formation of interlocked **45** (rather than non-interlocked isomer). The same study also disclosed the use of a labile stopper that could be substituted

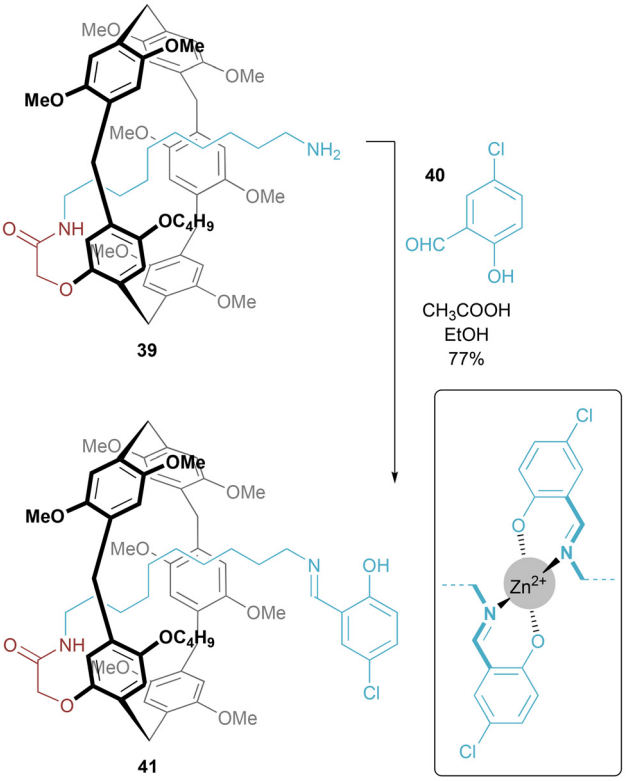

Fig. 24 Synthesis of salicylaldimine stoppered pillar[5]arene [1]rotaxane. *Inset*: proposed binding mode of Zn(II) cation.

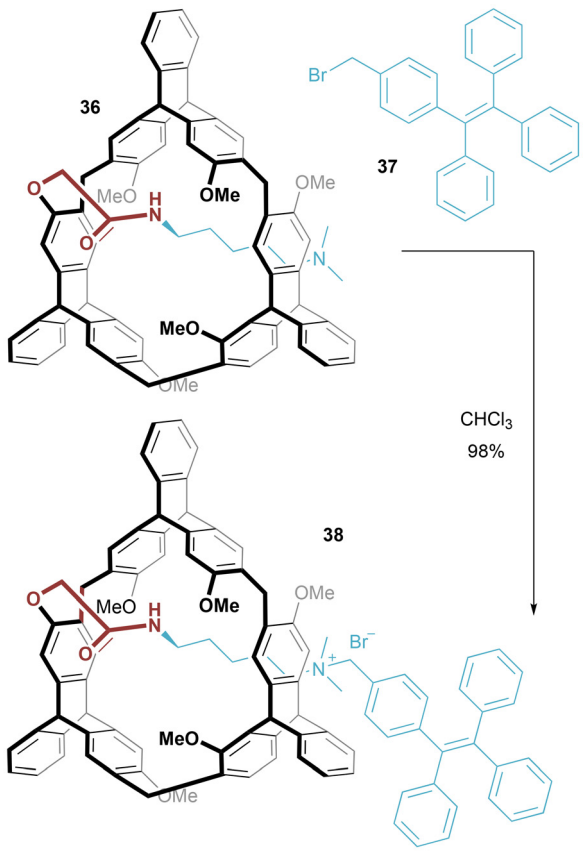

Fig. 23 Han and Chen's synthesis of a helic[6]arene-based [1]rotaxane.

without disruption of the mechanical bond. In the original report the full stereochemical assignment of [1]rotaxane **45** was not confirmed. In a follow-up paper, comparison of the experimentally recorded CD spectrum with computational calculations indicated that the (*S*, R_{mp}) diastereomer had been formed.[51]

[1]Rotaxanes prepared by clipping shut a macrocycle

Berna and co-workers used Leigh's hydrogen bond templated synthesis of rotaxanes to prepare benzylic amide [1]rotaxanes (such as **48**) *via* a self-templating clipping approach (Fig. 26).[52] Confirmation that no higher order (*i.e.* daisy chain) species were synthesized, was achieved by use of pulsed gradient spin echo NMR experiments to determine diffusion coefficients, as well as by checking the isotopic distribution in the mass spectrum. Disentangling was not observed in the ^{1}H NMR spectrum upon heating samples. Switching between extended and contracted lasso-like isomers was achieved by light-driven isomerization of the C=C double bond. In a follow-up paper, a *tert*-butyl group was added to the macrocycle, and in this case varying concentration of the reaction allowed for isolation of small amounts of daisy chain.[53]

[1]Rotaxane prepared by entanglement and stoppering an axle

Coutrot and co-workers reported the synthesis of a [1]rotaxane by entanglement followed by internal stoppering, deploying the electrostatically augmented hydrogen bond templation

Open Access Article. Published on 12 February 2025. Downloaded on 2/9/2026 7:36:12 PM.
This article is licensed under a Creative Commons Attribution 3.0 Unported Licence.

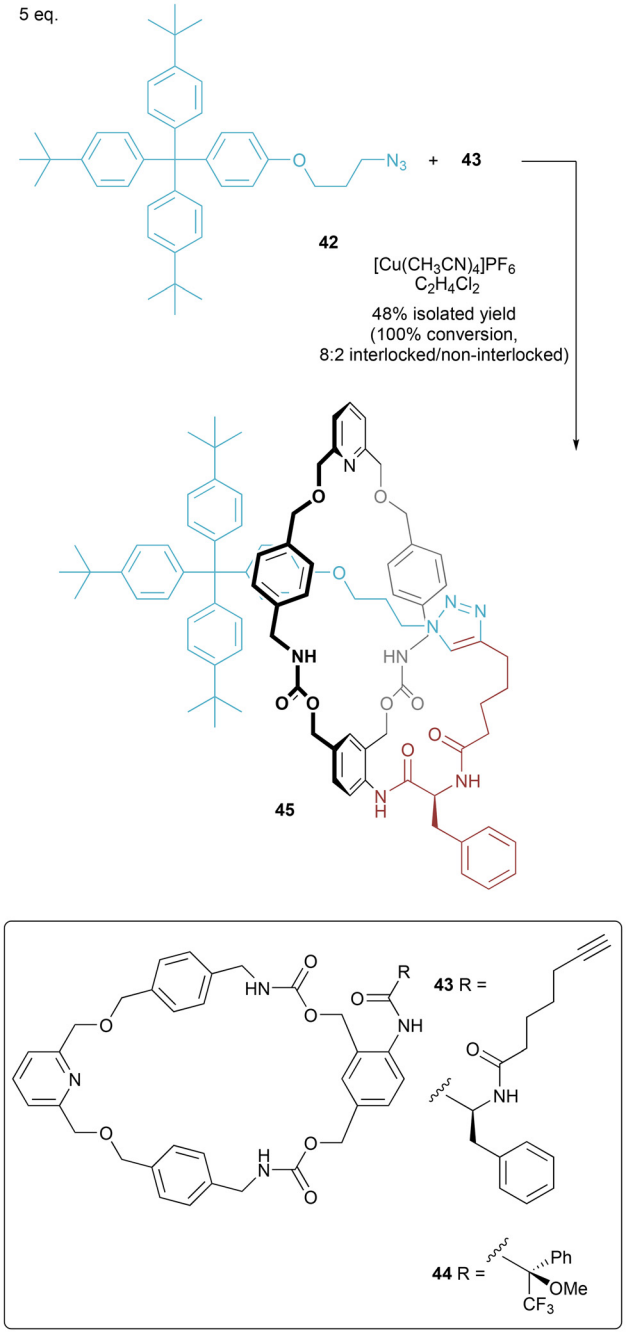

Fig. 25 Papot's active metal template synthesis of chiral [1]rotaxane.

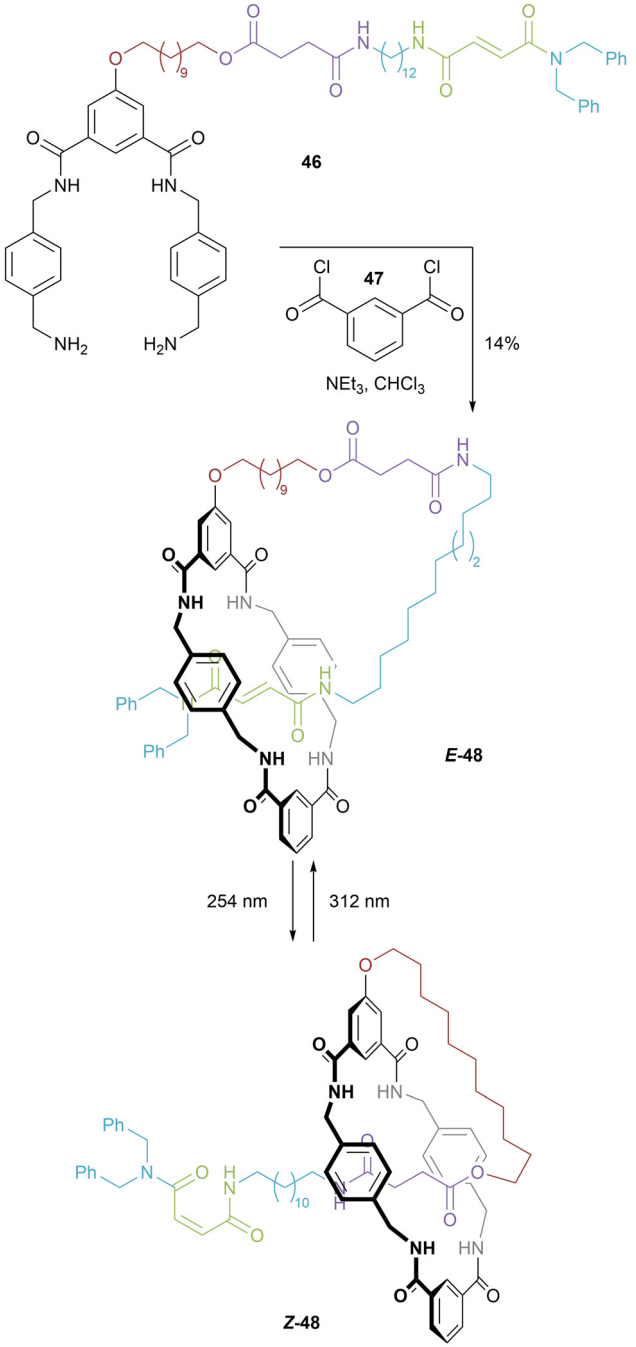

Fig. 26 Berna's synthesis of a hydrogen bond templated [1]rotaxane and light driven switching between extended and contracted conformations.

strategy of a protonated secondary ammonium axle component threaded through a crown ether (Fig. 27).[54] Removal of a Boc protecting group to generate **49** allows for self-entanglement to occur. Benzylation of the triazole secures the permanent [1]rotaxane structure of **51**, and provides the secondary station to allow for the pH-responsive shuttling of the molecular lasso.

[1]Rotaxane prepared by directed covalent approach

In contrast to non-covalent self-assembly used in the examples discussed so far, Hiratani's [1]rotaxane **52** was prepared by directed covalent synthesis, specifically aminolysis of bicyclic compound **50** (Fig. 28).[55] The permanent entanglement of the [1]rotaxane was verified by heating a sample of **52** in dimethyl sulfoxide. In **52**, fluorescence arises due to energy transfer from the naphthalenes of the macrocycle to the anthracene of the axle. In CH_2Cl_2/CH_3CN (9 : 1) solution, it was found that upon the addition of Li^+ (but neither Na^+ nor K^+) there was a

 This journal is © The Royal Society of Chemistry 2025

Open Access Article. Published on 12 February 2025. Downloaded on 2/9/2026 7:36:12 PM.
This article is licensed under a Creative Commons Attribution 3.0 Unported Licence.

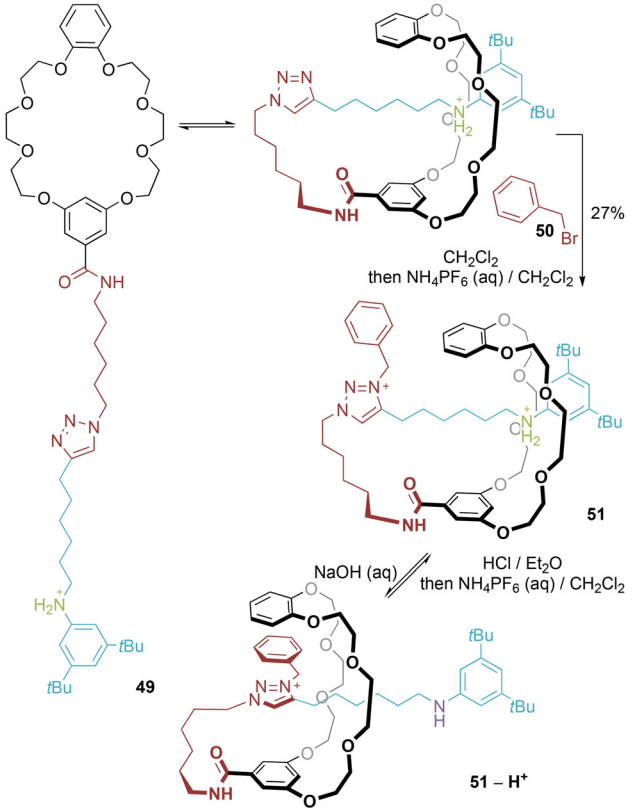

Fig. 27 Coutrot's synthesis of crown ether/secondary ammonium [1]rotaxane (NB: counter-anions not included to avoid ambiguity).

drastic enhancement of the fluorescence intensity – *i.e.* the [1]rotaxane acted as a selective sensor for lithium cations.

Molecular figures-of-eight

Molecular figures-of-eight have been significantly less common than either pretzelanes or [1]rotaxanes. However, they are of direct relevance for lasso peptides – *Class III* lasso peptides are molecular figures-of-eight. These species may be synthesized *via* a [2]rotaxane intermediate, followed by covalently linking the thread and macrocycle (Fig. 29a). An alternative route is through threading and linking (Fig. 29b). It is noted that at least two of the molecular figures-of-eight reported to date are devoid of "stoppers". The stability of the figure-of-eight conformation is attributed in these cases to restricted rotation at the point the linker is attached to macrocycle preventing disentanglement. Molecular figures-of-eight are also to be found as intermediates in the preparation of [2]rotaxanes by directed covalent synthesis.

Molecular figures-of-eight prepared *via* a [2]rotaxane scaffold

Once again, Vögtle and co-workers were pioneers in this field (Fig. 30).[56] Chemoselective alkylation of a [2]rotaxane by careful temperature control allowed for alkylation first at the more acidic sulfonamides and then at amides. The isolated product material consisted of multiple isomers, separable by

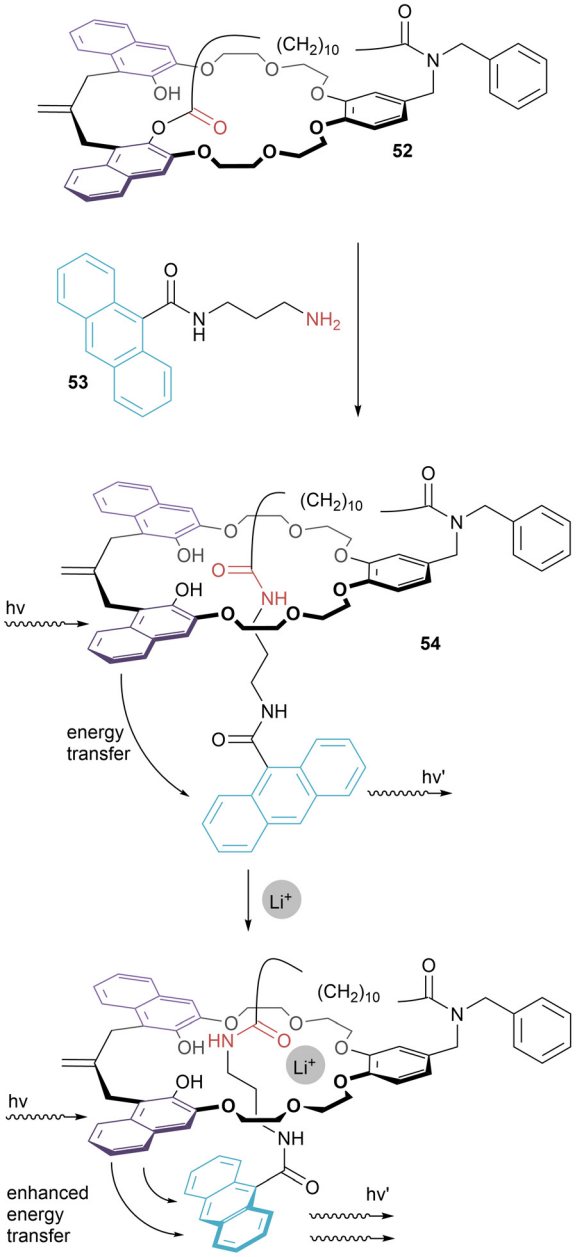

Fig. 28 Hiratani's [1]rotaxane: synthesis by directed covalent synthesis and proposed mode of lithium cation binding that leads to enhanced fluorescence.

HPLC in a ratio of 79 : 13 : 8. In contrast to [1]rotaxane **21**, figure-of-eight **55** possesses helical chirality. Enantiomers of the major isomer were resolved using chiral HPLC, allowing for the recording of CD spectra.

Molecular figure-of-eight prepared *via* threading and linking

Donor–acceptor molecular figure-of-eight **56** was prepared by CuAAC click chemistry (Fig. 31).[57] A mixture of two regioisomers was isolated in 12% yield, separable through iterative HPLC. In the original communication evidence is reported (hints of resonances in the ^{1}H NMR spectrum baseline) of

Open Access Article. Published on 12 February 2025. Downloaded on 2/9/2026 7:36:12 PM.
This article is licensed under a Creative Commons Attribution 3.0 Unported Licence.

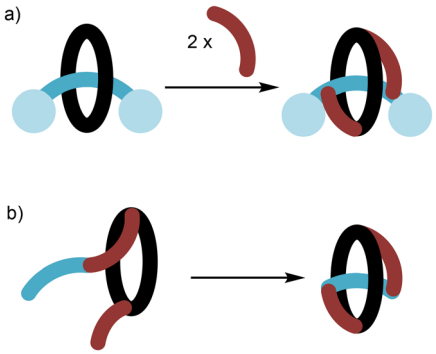

Fig. 29 Schematic representation of two synthetic routes to molecular figures-of-eight reported to date: (a) by double covalent linkage of a [2]rotaxane intermediate and (b) by threading and linking. NB: *in lieu* of stoppers, a molecular figure-of-eight may be permanently entangled by inclusion of sufficiently inflexible pivots.

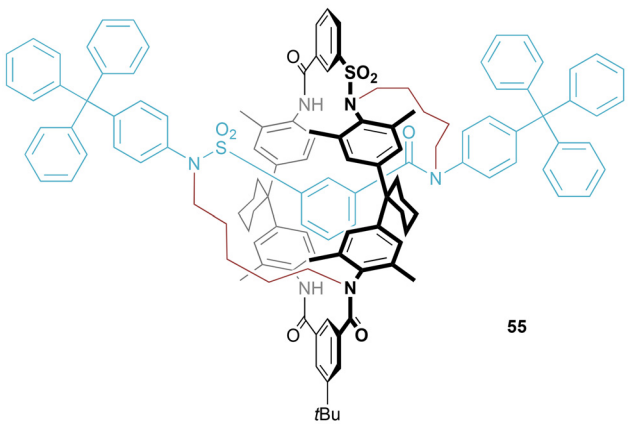

Fig. 30 Structure of Vögtle's molecular figure-of-eight.

minor conformations for both the *cis* and *trans* isomers. This was studied in further depth in a follow-up paper.[58]

Coutrot and co-workers have recently reported molecular figure-of-eight **57** (Fig. 32),[59] which is synthesized through threading and linking (once again utilizing the electrostatically augmented hydrogen bond templation of a protonated ammonium thread within the cavity of a dibenzo-24-crown-8) followed by ring closure (using a CuAAC reaction) and then methylation of the resulting triazole. Deprotonating (and Boc protecting) the ammonium centre, promotes shuttling so that the triazolium sits within the macrocycle cavity. Reprotonation (and removal of the Boc group) triggers a return to the initial state. As identified by the researchers this represents the first example of a synthetic molecular figure-of-eight designed to undergo stimuli-controlled molecular motion.

Molecular figures-of-eight arising as intermediates in the covalent directed synthesis of [2]rotaxanes

Molecular figure-of-eight **60** was a key intermediate in the synthesis of a [2]rotaxane as reported by Kawai and co-workers (Fig. 33).[60] The figure-of-eight was prepared in an excellent

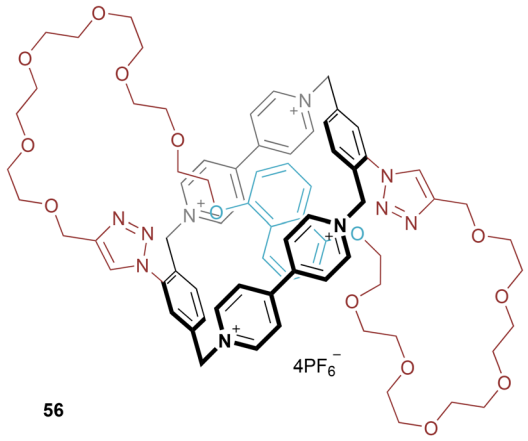

Fig. 31 Structure of Sauvage and Stoddart's molecular figure-of-eight (*trans* isomer depicted).

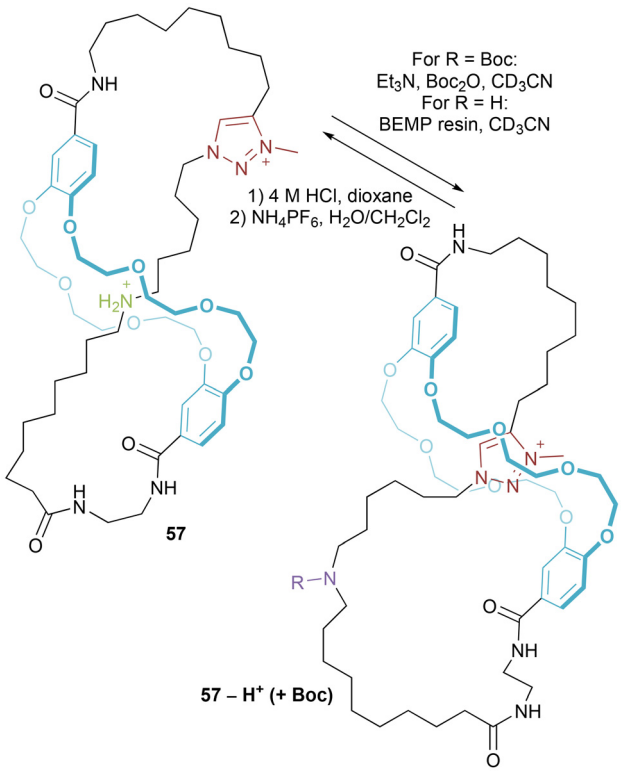

Fig. 32 Coutrot's molecular figure-of-eight which can shuttle between ammonium and triazolium stations (NB: counter-anions not included to avoid ambiguity).

95% yield from the corresponding bis-amine macrocycle and bis-aldehyde axle component. After removal of the silyl protecting groups and addition of bulky stopper groups, the imine bonds were hydrolyzed to furnish the desired [2]rotaxane.

Separately, van Maarseveen and co-workers prepared a molecular figure-of-eight (or, as alternatively termed by the authors, a "pre-rotaxane") **62** (Fig. 34). In this case, the researchers undertook macrocyclization (by Grubbs ring

This journal is © The Royal Society of Chemistry 2025

Open Access Article. Published on 12 February 2025. Downloaded on 2/9/2026 7:36:12 PM. This article is licensed under a Creative Commons Attribution 3.0 Unported Licence.

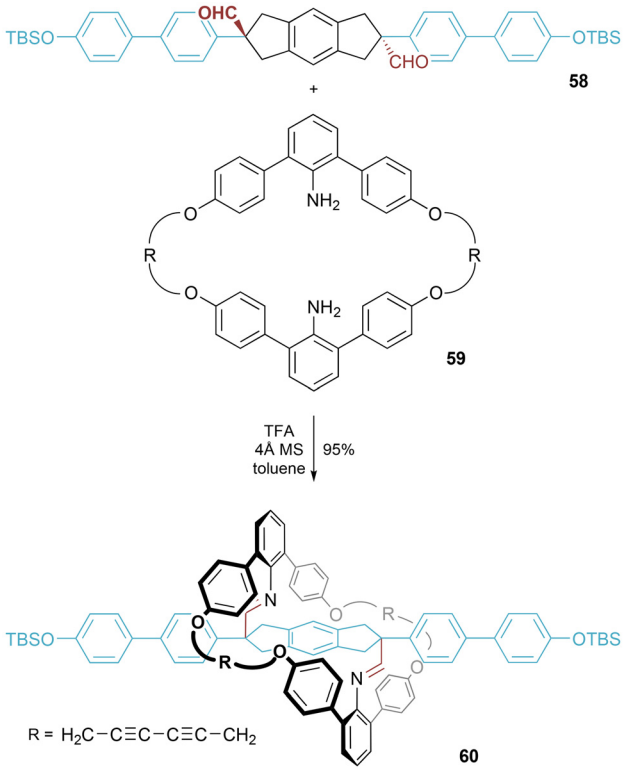

Fig. 33 Kawai's synthesis of a molecular figure-of-eight *en route* to a [2]rotaxane.

closing metathesis) around a bridging stoppered axle to generate the molecular figure-of-eight.[61] Saponification of the ester linkages followed by methyl ester formation on the liberated carboxylic acids led to an isolable [2]rotaxane.[62]

Synthetic analogues of lasso peptides

Lasso peptides are a structurally unusual class of peptides, that consist of a chain of amino acids with a "tail" threaded through a macrolactam "ring".[63] The permanently entangled [1]rotaxane structures of lasso peptides are ensured by the incorporation of amino acids with bulky side chains each side of the macrocyclic ring. They are well-known to evade degradation by many protease enzymes due to their entangled structures, and examples have been shown to possess bioactivity including antimicrobial activity,[64] receptor antagonism[65] and enzyme inhibition.[66] Studies have identified interesting thermal stability properties[67] and an example of a lasso peptide that acts as a thermal switch.[68]

The total synthesis of lasso peptides is non-trivial. Chen and co-workers reported the total synthesis of lasso peptide BI-32169 by use of a cryptand-imidazolium complex as a support (**63**, Fig. 35).[69] By attaching the C-terminus of a protected cysteine-alanine dipeptide to an imidazolium moiety, the peptide chain was able to form a host–guest complex with a bis-functionalized cryptand, with the N-terminus pointing out of the cryptand cavity. The amino acid chain was then built up stepwise; after ten further residues, the terminal

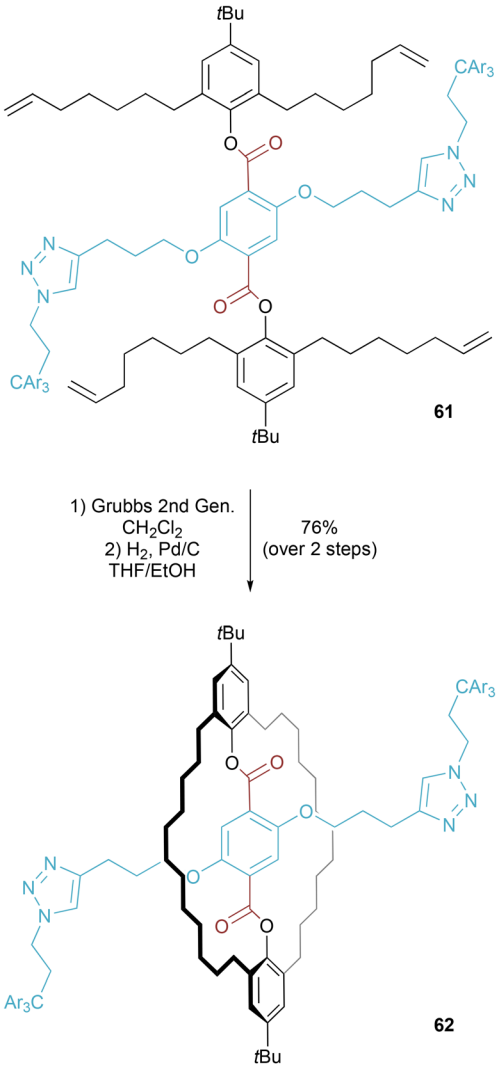

Fig. 34 van Maarseveen's synthesis of a molecular figure-of-eight *en route* to a [2]rotaxane.

serine was deprotected and linked to one side of the cryptand. Four more amino acid residues were added to the chain, finishing with a protected tryptophan, which was subsequently linked to the remaining free site on the cryptand. The final amino acid residues were added, which due to the three tethering sites on the chain, were preorganized allowing for formation of a macrocycle around the "thread" – generating a peptide bond between a terminal glycine and intermediate aspartic acid. Cleavage of the tethering groups liberated the targeted lasso peptide. Switching chirality of the complex and using D-amino acids, facilitated synthesis of the enantiomer of the naturally occurring lasso peptide. It was established that the synthetic, unnatural enantiomer had a significantly higher enzymatic stability compared to the natural lasso peptide.

Considering the challenges associated with the total synthesis of lasso peptides, and the discovery that the amino acids located in the "loop region" are important in determining the biological activity of a lasso peptide,[70] an alternative

Open Access Article. Published on 12 February 2025. Downloaded on 2/9/2026 7:36:12 PM.
This article is licensed under a Creative Commons Attribution 3.0 Unported Licence.

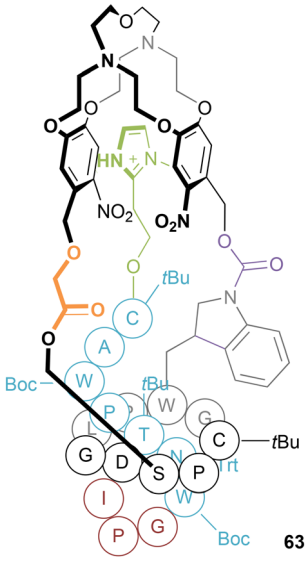

Fig. 35 Structure of Chen's cryptand-imidazolium complex with protected lasso peptide BI-32169 attached.

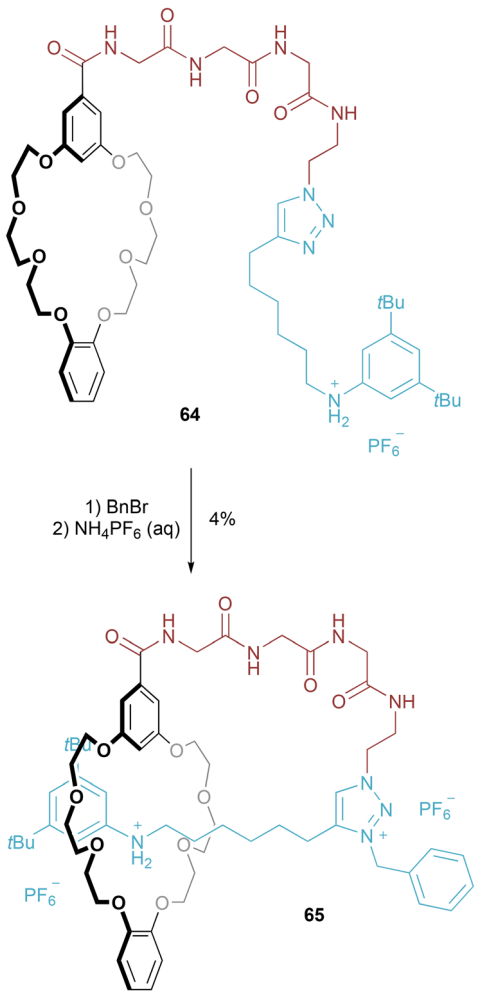

Fig. 36 Coutrot's synthesis of a switchable [1]rotaxane lasso peptide analogue.

supramolecular chemistry approach to accessing (analogues of) lasso peptides is to incorporate a relevant peptide sequence within the structure of a [1]rotaxane.

The first example of pursuing this approach was by Coutrot (Fig. 36).[71] [1]Rotaxane **65** – with a simple GlyGlyGly chain in the loop region – was prepared by application of the entanglement methodology described above for [1]rotaxane **51**. Unfortunately, in this case the isolated yield was very low (4%), due to particularly challenging chromatographic purification. Deprotonation of the anilinium triggers shuttling towards the triazolium station, resulting in a tightening of the [1]rotaxane conformation.

Subsequently, Bode also using the well-established crown ether/protonated secondary ammonium templation, synthesized a "parent" [2]rotaxane **66**, appended peptide sequence and then cyclized to form a set of [1]rotaxanes (*e.g.* **67**, Fig. 37).[72] When tested, the proteolytic stability of the synthetic lasso peptides were significantly more stable than their linear peptide analogues – indicating the [1]rotaxanes could prove to be effective scaffolds for functionally active peptides *in vivo*.

Evans and co-workers have since reported upon the proof-of-principle synthesis of a peptide-displaying [1]rotaxane **74** derived from a "parent" [2]rotaxane **71**, where the templated formation of the interlocked structure arises from hydrogen bonding by an isophthalamide macrocycle to an amide in the axle component (Fig. 38).[73]

Smith has reported upon molecular figures-of-eight displaying peptide sequences (Fig. 39).[74] A "parent" squaraine [2]rotaxane **75** was synthesized with alkyne and primary amine

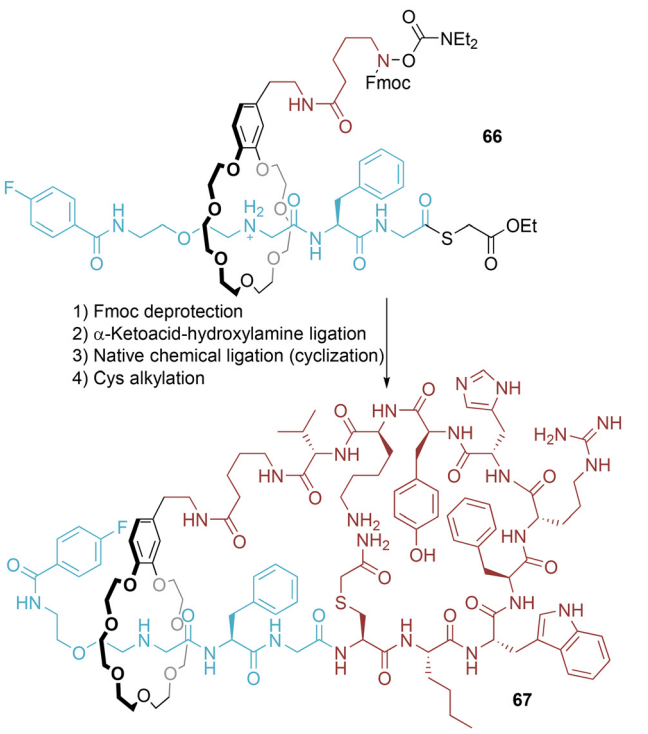

Fig. 37 Example of Bode's synthesis of a [1]rotaxane lasso peptide analogue.

This journal is © The Royal Society of Chemistry 2025

Open Access Article. Published on 12 February 2025. Downloaded on 2/9/2026 7:36:12 PM.
This article is licensed under a Creative Commons Attribution 3.0 Unported Licence.

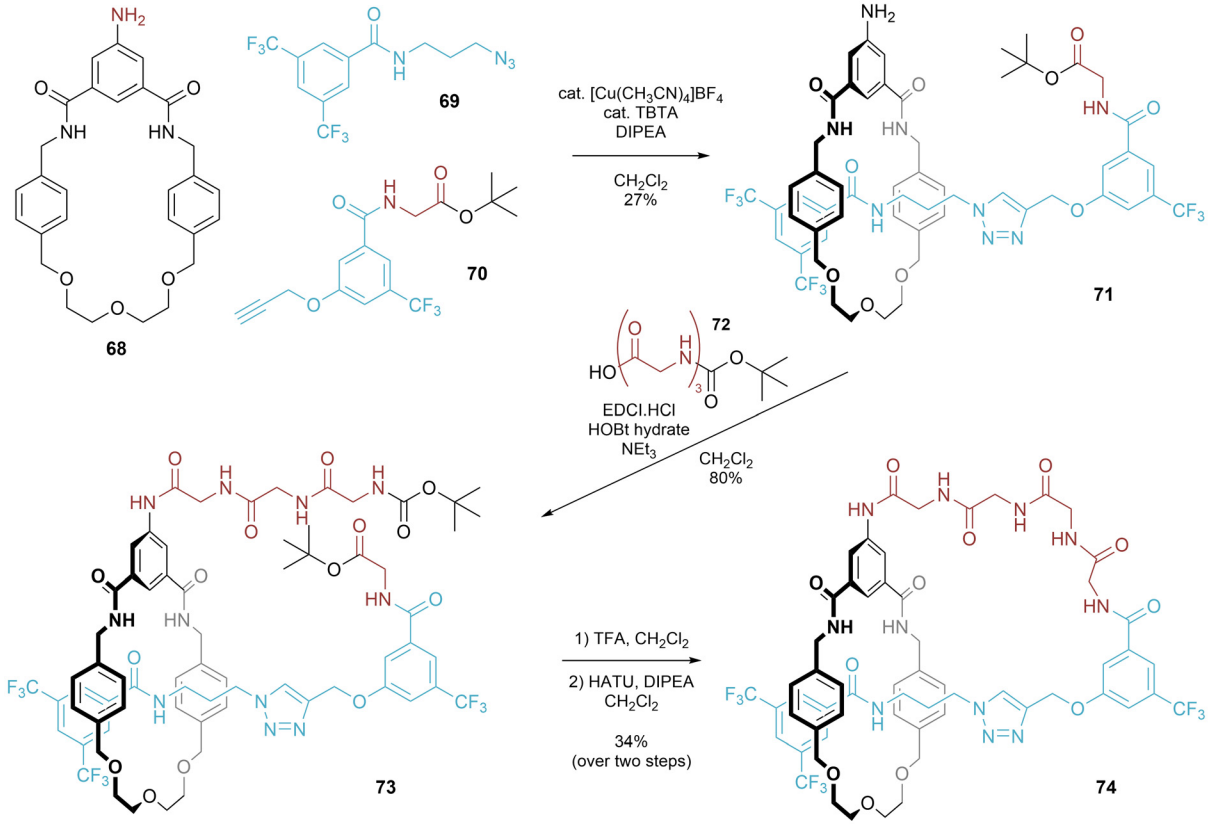

Fig. 38 Evans' synthesis of a [1]rotaxane lasso peptide analogue.

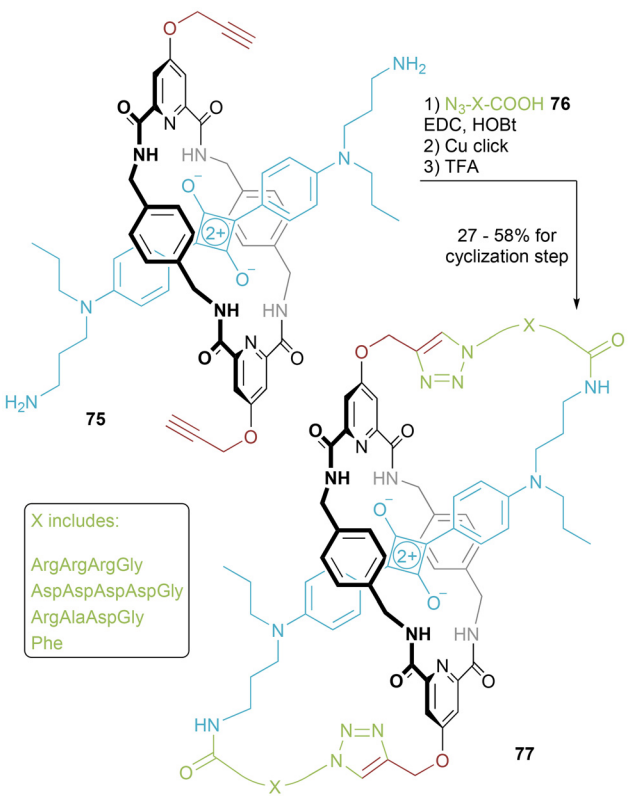

Fig. 39 Smith's synthesis of peptide containing molecular figures-of-eight.

functional handles. Appendage of amino acid sequences by amide formation followed by CuAAC "click" reactions (and cleavage of protecting groups) generates the target molecular figures-of-eight 77. The encapsulated squaraine motif is fluorescent and so resulting molecules may be used in conjunction with fluorescence microscopy and biological imaging. Incorporation of a cell-penetrating peptide within the "loop" regions targets the surface of cell plasma membranes. Alternatively, a bone-targeting peptide in the "loop" regions has been shown to selectively stain the skeleton of a mouse.

In follow-up, further squaraine-containing molecular figures-of-eight 77 were reported by Smith and co-workers.[75] By incorporating L-Phe into loops of one molecule and D-Phe into the loops of the other, chiral stereoisomers were isolated. Opposite Cotton effects were recorded in CD spectroscopy, that were not present in linear counterparts, indicating an enforced conformation for the molecular figures-of-eight. The fluorescence of the squaraine dye is unaffected by the change in handedness of incorporated amino acid, but excitingly the different stereoisomers localise in different cell areas.

Conclusions

Reflecting upon the covalently bridged MIMs discussed in this review, it is apparent that [1]rotaxanes are more frequently pre-

Open Access Article. Published on 12 February 2025. Downloaded on 2/9/2026 7:36:12 PM. This article is licensed under a Creative Commons Attribution 3.0 Unported Licence.

pared than pretzelanes or molecular figures-of-eight. While the scarcity of pretzelanes might be casually correlated to the greater number of [2]rotaxanes prepared to date compared to [2]catenanes, we highlight, however, that many [1]rotaxanes are prepared by threading and stoppering, rather than covalently linking the ring and axle of [2]rotaxanes. We also note the significant number of bridged MIMs prepared by directed covalent syntheses. Considering how bridging links naturally arise through such syntheses, we believe that directed covalent synthesis will continue to be an important strategy for preparing such species.

Perhaps unsurprisingly, there are plenty of examples of covalently bridged MIMs that exhibit stimuli controlled motion between different interlocked conformations. In contrast, while stereochemistry was a key aspect of Vögtle's pioneering investigations, the use of the chirality of such species has yet to blossom. We anticipate Papot's recent work on diastereoselective synthesis[50] may initiate the exploitation of chiral [1]rotaxanes in asymmetric synthetic applications.

Focusing on applications that have been demonstrated to date, there is undoubtedly a growing body of work on lasso peptide analogues – driven by the advantages arising from the entangled structure, that provides preorganization and metabolic protection of the peptide compared to open chain analogues.[69,72,74,75] However, there are also non-peptidic bridged MIMs being put to (at least) proof-of-principle functional applications. Hiratani's seminal lithium sensing [1]rotaxane[55] has now being joined – amongst others – by Lin's luminescent [1]rotaxanes.[42,43] Lin's systems exemplify how functional application may be derived from a bridged [1]rotaxane architecture, with variation in optical properties dependent on the different conformations arising from stimuli controlled switching.

Considering all the above, we are therefore confident of further exciting developments in the synthesis and application of covalently bridged MIMs in the years ahead.

Author contributions

Conceptualization: N. H. E.; funding acquisition: N. H. E.; writing: R. L. S. & N. H. E.

Data availability

No primary research results have been included and so there are no new data generated or analysed as part of this review.

Conflicts of interest

There are no conflicts to declare.

Acknowledgements

N. H. E. and R. L. S. acknowledge funding from the Leverhulme Trust through a Leverhulme Trust Research Project Grant (RPG-2019-315). N. H. E. also expresses appreciation to Lancaster University (Faculty of Science & Technology Research Grant), Joy Welch Educational Charitable Trust, EPSRC Directed Assembly Network (Seed Fund Grant awarded from EP/P007279/2) and Royal Society of Chemistry (Undergraduate Research Bursary U21-9259917127 for Jessica Hale) for funding of projects investigating covalently bridged interlocked molecules.

References

1 G. Gil-Ramírez, D. A. Leigh and A. J. Stephens, *Angew. Chem., Int. Ed.*, 2015, **54**, 6110–6150.
2 M. Xue, Y. Yang, X. Chi, X. Yan and F. Huang, *Chem. Rev.*, 2015, **115**, 7398–7501.
3 (*a*) D. A. Leigh, *Angew. Chem., Int. Ed.*, 2016, **55**, 14506–14508; (*b*) J.-P. Sauvage, *Angew. Chem., Int. Ed.*, 2017, **56**, 11080–11093; (*c*) J. F. Stoddart, *Angew. Chem., Int. Ed.*, 2017, **56**, 11094–11125.
4 J. T. Wilmore and P. D. Beer, *Adv. Mater.*, 2024, **36**, 2309098.
5 R. W. Heard, J. M. Suárez and S. M. Goldup, *Nat. Rev. Chem.*, 2022, **6**, 182–186.
6 (*a*) N. H. Evans, *Chem. – Eur. J.*, 2018, **24**, 3101–3112; (*b*) N. Pairault and J. Niemeyer, *Synlett*, 2018, **29**, 689–698; (*c*) E. M. G. Jamieson, F. Modicom and S. M. Goldup, *Chem. Soc. Rev.*, 2018, **47**, 5266–5311; (*d*) K. Nakazono and T. Takata, *Symmetry*, 2020, **12**, 144; (*e*) S. M. Goldup, *Acc. Chem. Res.*, 2024, **57**, 1696–1708.
7 J. E. Beves, B. A. Blight, C. J. Campbell, D. A. Leigh and R. T. McBurney, *Angew. Chem., Int. Ed.*, 2011, **50**, 9260–9327.
8 G. Barin, A. Coskin, M. M. G. Fouda and J. F. Stoddart, *ChemPlusChem*, 2012, **77**, 159–185.
9 N. H. Evans, *Eur. J. Org. Chem.*, 2019, 3320–3343.
10 For other examples of post-synthetic macrocyclization of rotaxanes: M. Gauthier, P. Waelès and F. Coutrot, *ChemPlusChem*, 2022, **87**, e202100458.
11 H. Martin-Gómez and J. Tulla-Puche, *Org. Biomol. Chem.*, 2018, **16**, 5065–5080.
12 P. Dabrowski-Tumanski and J. I. Sulkowska, *Proc. Natl. Acad. Sci. U. S. A.*, 2017, **114**, 3415–3420.
13 Molecular daisy chains arise from the self-complementary threading of multiple components consisting of an axle covalently linked to a macrocycle. Acyclic examples containing *n* components are termed "[*an*]daisy chain" while cyclic examples are termed "[*cn*]daisy chain". [*c2*] Daisy chains, otherwise known as Janus [2]rotaxanes, when dynamic are frequently termed "molecular muscles".
14 For a review on molecular daisy chains: E. Moulin, C. C. Carmona-Vargas and N. Giuseppone, *Chem. Soc. Rev.*, 2023, **52**, 7333–7358.
15 For a review on using DOSY NMR and ion mobility mass spectrometry to characterize [1]rotaxanes and molecular daisy chains: A. Saura-Sanmartin and C. A. Schalley, *Isr. J. Chem.*, 2023, **63**, e202300022.

 This journal is © The Royal Society of Chemistry 2025

Open Access Article. Published on 12 February 2025. Downloaded on 2/9/2026 7:36:12 PM. This article is licensed under a Creative Commons Attribution 3.0 Unported Licence.

16 Select examples of [*c2*]daisy chains/Janus [2]rotaxanes: (*a*) S. J. Rowan, S. J. Cantrill, J. F. Stoddart, A. J. P. White and D. J. Williams, *Org. Lett.*, 2000, **2**, 759–762; (*b*) M. C. Jiménez, C. Dietrich-Buchecker and J.-P. Sauvage, *Angew. Chem., Int. Ed.*, 2000, **39**, 3284–3287; (*c*) T. Hoshino, M. Miyauchi, Y. Kawaguchi, H. Yamaguchi and A. Harada, *J. Am. Chem. Soc.*, 2000, **122**, 9876–9877; (*d*) T. Fujimoto, Y. Sakata and T. Kaneda, *Chem. Commun.*, 2000, 2143–2144; (*e*) S. H. Ueng, S.-Y. Hsueh, C.-C. Lai, Y.-H. Liu, S.-M. Peng and S.-H. Chiu, *Chem. Commun.*, 2008, 817–819; (*f*) F. Coutrot, C. Romuald and E. Busseron, *Org. Lett.*, 2008, **10**, 3741–3744; (*g*) N. H. Evans and P. D. Beer, *Chem. – Eur. J.*, 2011, **17**, 10542–10546; (*h*) Z. Zhang, C. Han, G. Yu and F. Huang, *Chem. Sci.*, 2012, **3**, 3026–3031; (*i*) C. J. Bruns, J. Li, M. Frasconi, S. T. Schneebeli, J. Iehl, H. P. J. de Rouville, S. I. Stupp, G. A. Voth and J. F. Stoddart, *Angew. Chem., Int. Ed.*, 2014, **53**, 1953–1958; (*j*) A. Fernandez, E. M. Pineda, J. Ferrando-Soria, E. J. L. McInnes, G. A. Timco and R. E. P. Winpenny, *Chem. Commun.*, 2015, **51**, 11126–11129; (*k*) K. Iwaso, Y. Takashima and A. Harada, *Nat. Chem.*, 2016, **8**, 625–632; (*l*) J. C. Chang, S. H. Tseng, C.-C. Lai, Y.-H. Liu, S.-M. Peng and S.-H. Chiu, *Nat. Chem.*, 2017, **9**, 128–134; (*m*) J. M. Van Raden, N. N. Jarenwattananon, L. N. Zakharov and R. Jasti, *Angew. Chem., Int. Ed.*, 2020, **26**, 10205–10209.

17 Cyclization of [*c2*]daisy can lead to molecular double-lasso macrocycles: (*a*) C. Romuald, A. Ardá, C. Clavel, J. Jiménez-Barbero and F. Coutrot, *Chem. Sci.*, 2012, **3**, 1851–1857; (*b*) C. Romuald, G. Cazals, C. Enjalbal and F. Coutrot, *Org. Lett.*, 2013, **15**, 184–187; (*c*) S.-J. Rao, X.-H. Ye, Q. Zhang, C. Gao, W.-Z. Wang and D.-H. Qu, *Asian J. Org. Chem.*, 2018, **7**, 902–905.

18 R. Jäger, T. Schmidt, D. Karbach and F. Vögtle, *Synlett*, 1996, 723–725.

19 C. Yamamoto, Y. Okamoto, T. Schmidt, R. Jaeger and F. Vögtle, *J. Am. Chem. Soc.*, 1997, **119**, 10547–10548.

20 C. Reuter, A. Mohry, A. Sobanski and F. Vögtle, *Chem. – Eur. J.*, 2000, **6**, 1674–1682.

21 Q. Y. Li, E. Vogel, A. H. Parham, M. Nieger, M. Bolte, R. Fröhlich, P. Saarenketo, K. Rissanen and F. Vögtle, *Eur. J. Org. Chem.*, 2001, 4041–4049.

22 S. Shimada, K. Ishikawa and N. Tamaoki, *Acta Chem. Scand.*, 1998, **52**, 374–376.

23 Y. Liu, P. A. Bonvallet, S. A. Vignon, S. I. Khan and J. F. Stoddart, *Angew. Chem., Int. Ed.*, 2005, **44**, 3050–3055.

24 Y. Liu, S. A. Vignon, X. Zhang, K. N. Houk and J. F. Stoddart, *Chem. Commun.*, 2005, 3927–3929.

25 Y.-L. Zhao, A. Tabolsi and J. F. Stoddart, *Chem. Commun.*, 2009, 4844–4846.

26 Unidirectional motion in other catenanes has been demonstrated: (*a*) D. A. Leigh, J. K. Y. Wong, F. Dehez and F. Zerbetto, *Nature*, 2003, **424**, 174–179; (*b*) J. V. Hernández, E. R. Kay and D. A. Leigh, *Science*, 2004, **306**, 1532–1537; (*c*) S. Erbas-Cakmak, S. D. P. Fielden, U. Karaca, D. A. Leigh, C. T. McTernan, D. J. Tetlow and M. R. Wilson, *Science*, 2017, **358**, 340–343; (*d*) L. Zhang, Y. Qiu, W.-G. Liu, H. Chen, D. Shen, B. Song, K. Cai, H. Wu, Y. Jiao, Y. Feng, J. S. W. Seale, C. Pezzato, J. Tian, Y. Tan, X.-Y. Chen, Q.-H. Guo, C. L. Stern, D. Philp, R. D. Astumian, W. A. Goddard III and J. F. Stoddart, *Nature*, 2023, **613**, 280–286; (*e*) A. Li, Z. Du, S. Zhang, J. Xie, X. Li, Q. Chen, Y. Tang, J. Chen and K. Zhu, *Chem. Sci.*, 2024, **15**, 14721–14725.

27 M. Han, H.-Y. Zhang, L.-X. Yang, Z.-J. Ding, R.-J. Zhuang and Y. A. Liu, *Eur. J. Org. Chem.*, 2011, 7271–7277.

28 (*a*) G. Schill and A. Lüttringhaus, *Angew. Chem., Int. Ed. Engl.*, 1964, **3**, 546–547; (*b*) G. Schill, *Chem. Ber.*, 1967, **100**, 2021–2037.

29 Ö. Ünsal and A. Godt, *Chem. – Eur. J.*, 1999, **5**, 1728–1733.

30 M. D. Cornelissen, S. Pilon and J. H. van Maarseveen, *Synthesis*, 2021, **53**, 4527–4548.

31 S. Pilon, S. I. Jørgensen and J. H. van Maarseveen, *Chem. – Eur. J.*, 2021, **27**, 2310–2314.

32 Z. Xue and M. F. Mayer, *J. Am. Chem. Soc.*, 2010, **132**, 3274–3276.

33 (*a*) F. Coutrot, in *Single Molecular Machines and Motors* ed. C. Joachim and G. Rapenne, Springer International Publishing, Switzerland, 2015, pp. 35–64; (*b*) P. Waelès, C. Clavel, K. Fournel-Marotte and F. Coutrot, *Chem. Sci.*, 2015, **6**, 4828–4836.

34 R. Jäger, M. Händel, J. Harren, K. Rissanen and F. Vögtle, *Liebigs Ann.*, 1996, 1201–1207.

35 C. Reuter, C. Seel, M. Nieger and F. Vögtle, *Helv. Chim. Acta*, 2000, **83**, 630–640.

36 Q. Zhou, P. Wei, Y. Zhang, Y. Yu and X. Yan, *Org. Lett.*, 2013, **15**, 5350–5353.

37 H. Onagi, C. J. Blake, C. J. Easton and S. F. Lincoln, *Chem. – Eur. J.*, 2003, **9**, 5978–5988.

38 H. Li, H. Zhang, Q. Zhang, Q.-W. Zhang and D.-H. Qu, *Org. Lett.*, 2012, **14**, 5900–5903.

39 H. Li, J. N. Zhang, W. Zhou, H. Zhang, Q. Zhang, D.-H. Qu and H. Tian, *Org. Lett.*, 2013, **15**, 3070–3073.

40 F. Coutrot and E. Busseron, *Chem. – Eur. J.*, 2008, **14**, 4784–4787.

41 J.-J. Yu, L.-Y. Zhao, Z.-T. Shi, Q. Zhang, G. London, W.-J. Liang, C. Gao, M.-M. Li, X.-M. Cao, H. Tian, B. L. Feringa and D.-H. Qu, *J. Org. Chem.*, 2019, **84**, 5790–5802.

42 T. M. Khang, P. Q. Nhien, T. T. K. Cuc, C.-C. Weng, C.-H. Wu, J. I. Wu, B. T. B. Hue, Y.-K. Li and H.-C. Lin, *Small*, 2023, **19**, 2205597.

43 N. T. Trung, C.-H. Chiu, T. T. K. Cuc, T. M. Khang, S. Jalife, P. Q. Nhien, B. T. B. Hue, J. I. Wu, Y.-K. Li and H.-C. Lin, *Adv. Mater.*, 2024, **36**, 2311789.

44 X. Ma, D. Qu, F. Ji, Q. Wang, L. Zhu, Y. Xu and H. A. Tian, *Chem. Commun.*, 2007, 1409–1411.

45 A further contemporaneous example of a cyclodextrin [1]rotaxane prepared by threading and stoppering: P. Franchi, M. Fanì, E. Mezzina and M. Lucarini, *Org. Lett.*, 2008, **10**, 1901–1904.

46 X. Song, X. Zhu, S. Qiu, W. Tian and M. Liu, *Angew. Chem., Int. Ed.*, 2022, **61**, e202208574.

Open Access Article. Published on 12 February 2025. Downloaded on 2/9/2026 7:36:12 PM. This article is licensed under a Creative Commons Attribution 3.0 Unported Licence.

47 X.-S. Du, Y. Han and C.-F. Chen, *Chem. – Eur. J.*, 2022, **28**, e202104024.
48 L. Ma, R. Tang, Y. Zhou, J. Bei, Y. Wang, T. Chen, C. Ou, Y. Han, C.-G. Yan and Y. Yao, *Chem. Commun.*, 2022, **58**, 8978–8981.
49 Further examples of pillar[5]arene-based [1]rotaxanes: (*a*) X.-S. Du, C.-Y. Wang, Q. Jia, R. Deng, H.-S. Tian, H.-Y. Zhang, K. Meguellati and Y.-W. Yang, *Chem. Commun.*, 2017, **53**, 5326–5329; (*b*) H. Tian, R. Li, P.-H. Lin and K. Maguellati, *New J. Chem.*, 2020, **44**, 10628–10632.
50 N. Pairault, A. Bessaguet, R. Barat, L. Frédéric, G. Pieters, J. Crassous, I. Opalinski and S. Papot, *Chem. Sci.*, 2021, **12**, 2521–2526.
51 A. R. Puente, A. Bessaguet, N. Pairault, G. Pieters, J. Crassous, P. L. Polavarapu, I. Opalinski and S. Papot, *Chirality*, 2021, **33**, 773–782.
52 A. Saura-Sanmartin, A. Martinez-Cuezva, A. Pastor, D. Bautista and J. Berna, *Org. Biomol. Chem.*, 2018, **16**, 6980–6987.
53 A. Saura-Sanmartin, A. Pastor, A. Martinez-Cuezva and J. Berna, *Chem. Commun.*, 2022, **58**, 290–293.
54 C. Clavel, C. Romuald, E. Brabet and F. Coutrot, *Chem. – Eur. J.*, 2013, **19**, 2982–2989.
55 K. Hiratani, M. Kaneyama, Y. Nagawa, E. Koyama and M. Kanesato, *J. Am. Chem. Soc.*, 2004, **126**, 13568–13569.
56 C. Reuter, W. Wienand, C. Schmuck and F. Vögtle, *Chem. – Eur. J.*, 2001, **7**, 1728–1733.
57 M. M. Boyle, R. S. Forgan, D. C. Friedman, J. J. Gassensmith, R. A. Smaldone, J. F. Stoddart and J.-P. Sauvage, *Chem. Commun.*, 2011, **47**, 11870–11872.
58 M. M. Boyle, J. J. Gassensmith, A. C. Whalley, R. S. Forgan, R. A. Smaldone, K. J. Hartlieb, A. K. Blackburn, J.-P. Sauvage and J. F. Stoddart, *Chem. – Eur. J.*, 2012, **18**, 10312–10323.
59 M. Gauthier, J. Fournel-Marotte, C. Clavel, P. Waelès, P. Laurent and F. Coutrot, *Angew. Chem., Int. Ed.*, 2023, **62**, e202310643.
60 H. Kawai, T. Umehara, K. Fujiwara, T. Tsuji and T. Suzuki, *Angew. Chem., Int. Ed.*, 2006, **45**, 4281–4286.
61 L. Steemers, M. J. Wanner, A. W. Ehlers, H. Hiemstra and J. H. van Maarseveen, *Org. Lett.*, 2017, **19**, 2342–2345.
62 Further example of a molecular figure-of-eight as precursor to [2]rotaxane: C. Schweez, P. Shushkov, S. Grimme and S. Höger, *Angew. Chem., Int. Ed.*, 2016, **55**, 3328–3333.
63 (*a*) M. O. Maksimov, S. J. Pan and A. J. Link, *Nat. Prod. Rep.*, 2012, **29**, 996–1006; (*b*) J. D. Hergemann, H. Zimmermann, X. Xie and M. A. Marahiel, *Acc. Chem. Res.*, 2015, **48**, 1909–1919.
64 (*a*) R. A. Salomón and R. N. Farías, *J. Bacteriol.*, 1992, **174**, 7428–7435; (*b*) M. Iwatsuki, H. Tomoda, R. Uchida, H. Gouda, S. Hirono and S. Ōmura, *J. Am. Chem. Soc.*, 2006, **128**, 7486–7491; (*c*) T. A. Knappe, U. Linne, S. Zirah, S. Rebuffat, X. Xie and M. A. Marahiel, *J. Am. Chem. Soc.*, 2008, **130**, 11446–11454; (*d*) W. L. Cheung-Lee, M. E. Parry, A. J. Cartagena, S. A. Darst and A. J. Link, *J. Biol. Chem.*, 2019, **294**, 6822–6830.
65 (*a*) R. Katahira, K. Shibata, M. Yamasaki, Y. Matsuda and M. Yoshida, *Bioorg. Med. Chem.*, 1995, **3**, 1273–1280; (*b*) T. A. Knappe, U. Linne, X. Xie and M. A. Marahiel, *FEBS Lett.*, 2010, **584**, 785–789.
66 (*a*) G. Helynck, C. Dubertet, J. F. Mayaux and J. Leboul, *J. Antibiot.*, 1993, **46**, 1756–1757; (*b*) N. R. Braffman, F. J. Piscotta, J. Hauver, E. A. Campbell, A. J. Link and S. A. Darst, *Proc. Natl. Acad. Sci. U. S. A.*, 2019, **116**, 1273–1378.
67 J. D. Hegemann, *ChemBioChem*, 2020, **21**, 7–18.
68 C. Zong, M. J. Wu, J. Z. Qin and A. J. Link, *J. Am. Chem. Soc.*, 2017, **139**, 10403–10409.
69 M. Chen, S. Wang and X. Yu, *Chem. Commun.*, 2019, **55**, 3323–3326.
70 T. A. Knappe, F. Manzenrieder, C. Mas-Moruno, U. Linne, F. Sasse, H. Kessler, X. Xie and M. A. Marahiel, *Angew. Chem., Int. Ed.*, 2011, **50**, 8714–8717.
71 C. Clavel, K. Fournel-Marotte and F. Coutrot, *Molecules*, 2013, **18**, 11553–11575.
72 F. Saito and J. W. Bode, *Chem. Sci.*, 2017, **8**, 2878–2884.
73 M. J. Young, G. R. Akien and N. H. Evans, *Org. Biomol. Chem.*, 2020, **18**, 5203–5209.
74 C. Zhai, C. L. Schreiber, S. Padilla-Coley, A. G. Oliver and B. D. Smith, *Angew. Chem., Int. Ed.*, 2020, **59**, 23740–23747.
75 C. L. Schreiber, C. Zhai and B. D. Smith, *Org. Biomol. Chem.*, 2021, **19**, 3213–3219.

 This journal is © The Royal Society of Chemistry 2025